Tritium Permeability of Incoloy 800H and Inconel 617

P. Calderoni
P. Humrickhouse
R. Pawelko
M. Shimada
P. Winston

September 2011

INL

Idaho National Laboratory

Tritium Permeability of Incoloy 800H and Inconel 617

P. Calderoni, P. Humrickhouse, R. Pawelko, M. Shimada and P. Winston

September 2011

Idaho National Laboratory
Next Generation Nuclear Plant Project
Idaho Falls, Idaho 83415

http://www.inl.gov

Next Generation Nuclear Plant Project

Tritium Permeability of Incoloy 800H and Inconel 617

INL/EXT-11-23265
Revision 0
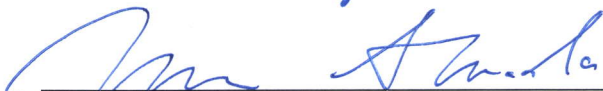
September 2011

Approved by:

_____   9-8-11
P. Humrickhouse   Date

_____   9/8/2-11
M. Shimada   Date
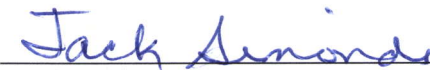
_____   9/14/2011
J. Simonds   Date
Manager, AGR Fuel Development Program

_____   9/8/2011
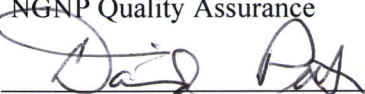K. J. Armour   Date
NGNP Quality Assurance

_____   9/14/2011
D. A. Petti   Date
Director, VHTR Technology Development Office

ABSTRACT

Design of the Next Generation Nuclear Plant (NGNP) reactor and its high-temperature components requires information regarding the permeation of fission-generated tritium and hydrogen product through candidate heat exchanger alloys. Release of fission-generated tritium to the environment and the potential contamination of the helium coolant by permeation of product hydrogen into the coolant system represent safety basis and product contamination issues. Of the three potential candidates for high-temperature components of the NGNP reactor design, only permeability for Incoloy 800H has been well documented. Hydrogen permeability data have been published for Inconel 617, but only in two literature reports and for partial pressures of hydrogen greater than one atmosphere, far higher than anticipated in the NGNP reactor.

To support engineering design of the NGNP reactor components, the tritium permeability of Inconel 617 and Incoloy 800H was determined using a measurement system designed and fabricated at Idaho National Laboratory (INL). The tritium permeability of Incoloy 800H and Inconel 617 was measured in the temperature range 650 to 950°C and at primary concentrations of 1.5 to 6 parts per million volume tritium in helium (partial pressures of 10^{-6} atm—three orders of magnitude lower partial pressures than used in the hydrogen permeation testing). The measured tritium permeability of Incoloy 800H and Inconel 617 deviated substantially from the values measured for hydrogen. This may be due to instrument offset, system absorption, and the presence of competing quantities of hydrogen, surface oxides, or other phenomena. Due to the challenge of determining the chemical composition of a mixture with such a low hydrogen isotope concentration, no categorical explanation of this offset has been developed.

As a result, the permeation measurements made in hydrogen should be considered the valid data set for use in any assessment until the issues associated with the tritium measurements can be resolved. If funding is available in the future the cause of the anomalous tritium permeability will be investigated.

CONTENTS

FIGURES

TABLES

ACRONYMS

DOE	Department of Energy
DU	depleted uranium
INL	Idaho National Laboratory
NGNP	Next Generation Nuclear Plant
NIST	National Institute for Standards and Technology
PVT	pressure-volume-temperature
SAS	storage and assay system
SEM	scanning electron microscopy
UHP	utra high purity
VHTR	very high temperature reactor

Tritium Permeability of Incoloy 800H and Inconel 617

1. INTRODUCTION

The U.S. Department of Energy (DOE) has selected the very high temperature reactor (VHTR) concept for the Next Generation Nuclear Plant (NGNP). Conceptually, NGNP can produce electricity, generate hydrogen, and provide industrial process heat at temperatures up to 950°C. The NGNP design is conceptually a graphite reactor core in which the primary coolant is recirculating helium gas. The very high planned outlet temperatures impose severe service requirements on the structural components of the reactor and intermediate heat exchanger. The need for resistance to high temperature creep severely limits candidate alloys to high-nickel alloys. Presently, alloys that are candidates for high-temperature structural components are Incoloy 800H, Inconel 617, and Haynes 230.[1]

Containment of fission products is a paramount concern in the operation of a nuclear reactor. The containment of tritium, a gaseous fission product, is of special concern in NGNP because of its high relative mobility in the core at the high operating temperatures. Tritium will be produced in the NGNP reactor as a tertiary fission product and by activation of graphite core contaminants such as lithium (Li-6 and Li-7) of the helium isotope, He-3, which is naturally present in the helium gas coolant, as well as the boron in the B_4C burnable poison. Tritium is a radioactive isotope of hydrogen. It is an internal radiological hazard to humans and has a release that is stringently limited by federal regulations. Because of its potentially high mobility at the reactor outlet temperatures, the tritium poses a risk of permeating through the walls of the intermediate heat exchanger and steam generator systems, potentially contaminating the environment and the hydrogen product. Therefore, the stringent environmental regulatory limits require that the design of the core and the plant system effectively contain the tritium produced by fission and activation.

The design of an acceptable containment system requires the selection of materials that allow the control of fission product permeation. This is particularly important for the alloys comprising the high-temperature service components of the NGNP system such as the intermediate heat exchanger and the steam generator. Most gases, including hydrogen and tritium, have a finite permeation rate through materials, which generally increases exponentially with temperature. The magnitude of the permeation rate at any temperature is a function of the activation energy and the permeation constant (the Arrhenius frequency factor or pre-exponential factor), which are characteristics determined by the elemental composition, phase composition, microstructure, and surface coatings of the alloys and materials. The characterization of the permeation process is therefore essential for the design of control systems that ensure that emission limits are satisfied under all credible circumstances.

The permeation of hydrogen through the candidate alloys has been investigated during FY 2010, and permeation of tritium in FY 2011. Of the three candidate high-nickel alloys, only Incoloy 800/800H has been significantly tested for permeation, with several reports in the literature (Figure 1).[2,3,4,5,6,7,8,9,10] By comparison, only two groups have reported hydrogen permeability data for Inconel 617 and none for Haynes 230.[5,7] (Of these, tritium permeation has been reported only for Incoloy 800/800H, and only by two groups.) The activation energy for hydrogen permeation, Q (in units of kcal/mol), and the Arrhenius pre-exponential term, K_0 (in units of cm^3 [standard temperature and pressure (STP; 0°C, 1 atmosphere)] hydrogen/cm·sec·$atm^{1/2}$)[a] are given in Table 1 for Incoloy 800/800H and Inconel 617, along with the applicable temperature and pressure ranges for the literature data. No permeability data for Haynes 230 have been found. As indicated in Table 1, the literature data generally pertain to hydrogen partial pressures greater than 0.1 atm, with the exception of the data of Roehrig et al.,[4] and all are substantially

---

a. These choices of units were made for ease of comparison with literature data that also use them. To convert to mol/(m•s•$Pa^{1/2}$), divide by 7.66e4.

higher than hydrogen and tritium pressures typical of the steady-state conditions within a VHTR core, at which a different permeation mechanism may operate. These data must be generated experimentally to support the design of the NGNP systems. Because high temperature permeation measurement systems are not available commercially, a system suitable for the task was designed and built as part of the permeation measurement task.
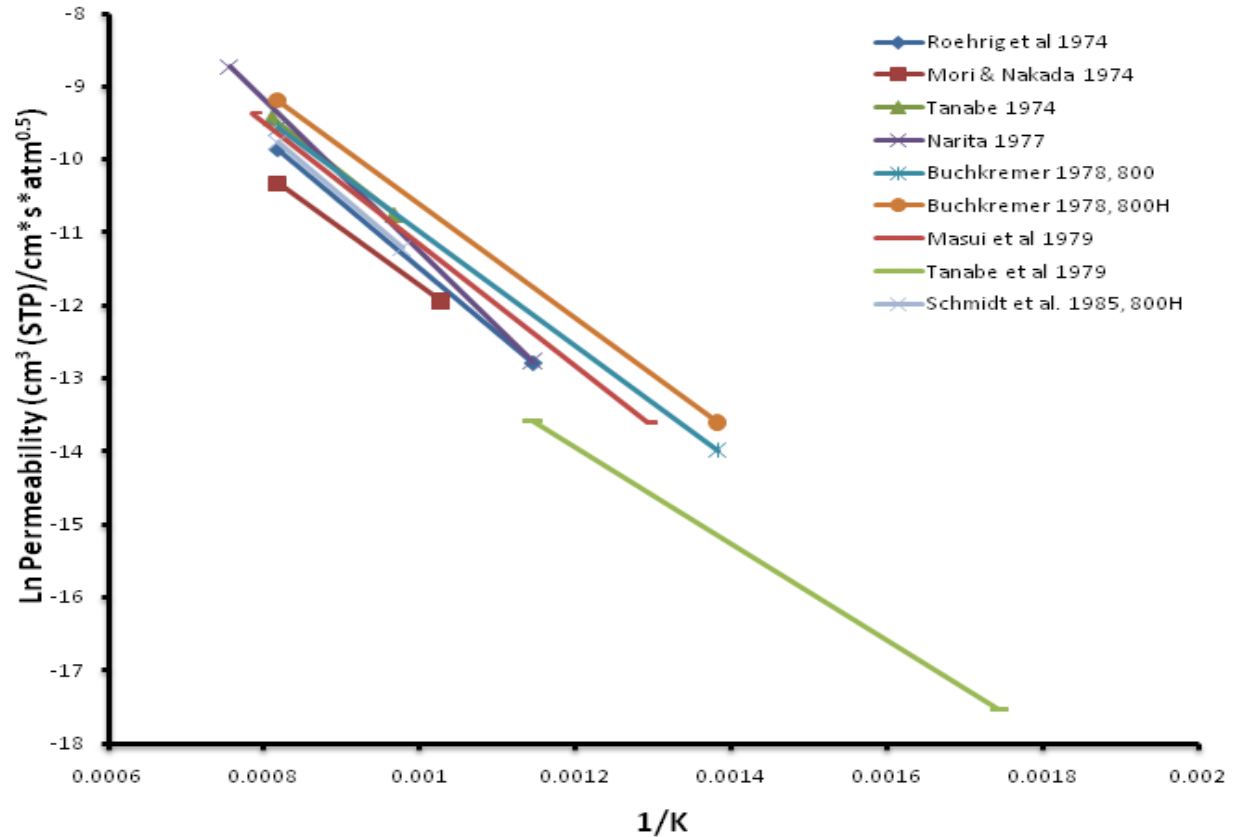
Figure 1. Summary of literature data for hydrogen permeability through Incoloy 800/800H.

Table 1. Literature values of the Arrhenius pre-exponential and activation energy for hydrogen permeation through Incoloy 800/800H, Inconel 617, and Haynes 230.

K_0 cm³ H₂ (STP)/cm·sec·atm$^{1/2}$	Q kcal/mol	Temp. Range °C	Pressure Range atm	References
Incoloy 800/800H, Hydrogen Permeability				
3.59×10^{-1} *	21.6	650–950	0.001–0.01	11
7.39×10^{-2}	17.7	600–950	$5 \times 10^{-4} - 0.5$	4
1.76×10^{-2}	15.3	700–950	1–5	2
7.58×10^{-2}	16.8	760–960	1	8
4.03×10^{-1}	20.6	600–1050	1–10	7
4.02×10^{-2}	15.5	450–950	5–10	9,12
5.90×10^{-2} *	15.5 *	450–950	5–10	9,12
6.02×10^{-2}	16.6	500–1000	0.1–1	3
2.44×10^{-3}	13.1	300–600	0.13–0.8	6
9.24×10^{-2} *	18.0 *	750–950	<40	5
Incoloy 800/800H, Tritium Permeability				
2.60×10^{-2}	16.1	350–750	2 ppm ³H, 1 atm H₂	13, 14
1.50×10^{-3}	13.5	750–950	1×10^{-4}	5
Inconel 617, Hydrogen Permeability				
5.39×10^{-1}	21.3	650–950	0.001–0.01	11
2.28×10^{-1}	18.9	600–1050	1–10	7
1.39×10^{-1}	19.8	750–950	< 40	5
Haynes 230, Hydrogen Permeability				
No reports	No reports			

* Data for Incoloy 800H

2. OBJECTIVES OF THE RESEARCH

The objective of the Fission Product Transport-Tritium Permeation work is to experimentally determine the permeation rates of tritium through the candidate alloys for NGNP structural components, which include Incoloy 800H, Inconel 617, and Haynes 230. Due to time constraints and reevaluation of the expected operating conditions, 800H and 617 were tested in preference to Haynes 230. The work consisted of three phases: (1) acquisition and transfer of a specific quantity of tritium gas into the tritium permeation glovebox, (2) determination of the permeability of tritium through the two candidate alloys at low partial pressures; and (3) determination of the tritium permeation constants through the same alloys. The permeability measurement system was designed for operation with hydrogen or tritium, either as a single-pass or as a recirculation system, and operating at temperatures in the range 650 to 950°C. The system was used in FY 2010 to test the hydrogen permeability of Incoloy 800H, Inconel 617 and Haynes 230. The tritium permeability of Incoloy 800H and Inconel 617 was measured in the range 650 to 950°C at concentrations varying from 1.5 to 6 ppmv tritium in helium.

This report summarizes the measurement of tritium permeability at high temperatures through the two candidate alloys.

3. DESCRIPTION OF THE MEASUREMENT SYSTEM, SAMPLES, AND TEST PARAMETERS

3.1 Permeation Measurement System

The measurement system, shown by the simplified diagram in Figure 2(a) and also by the detailed diagram in Figures 2(b) and 2(c), consists of two counter-flowing gas flow loops separated by the heated tubular test sample. The thin-walled tubular sample, mounted within a sealed quartz sample chamber, is the permeation interface separating the counter-flowing helium gas streams of the primary and secondary gas loops. The probe gas mixture (helium and tritium) in the primary gas loop flows through the bore of the tubular test sample, while the helium of the secondary gas loop, which includes the volume of the test chamber, flows over the external surface of the tubular sample to sweep away the permeated gas. The concentration of the permeated hydrogen gas in the helium of the secondary gas loop is measured by a quadrupole mass spectrometer and, in tritium measurements, by an ion chamber.
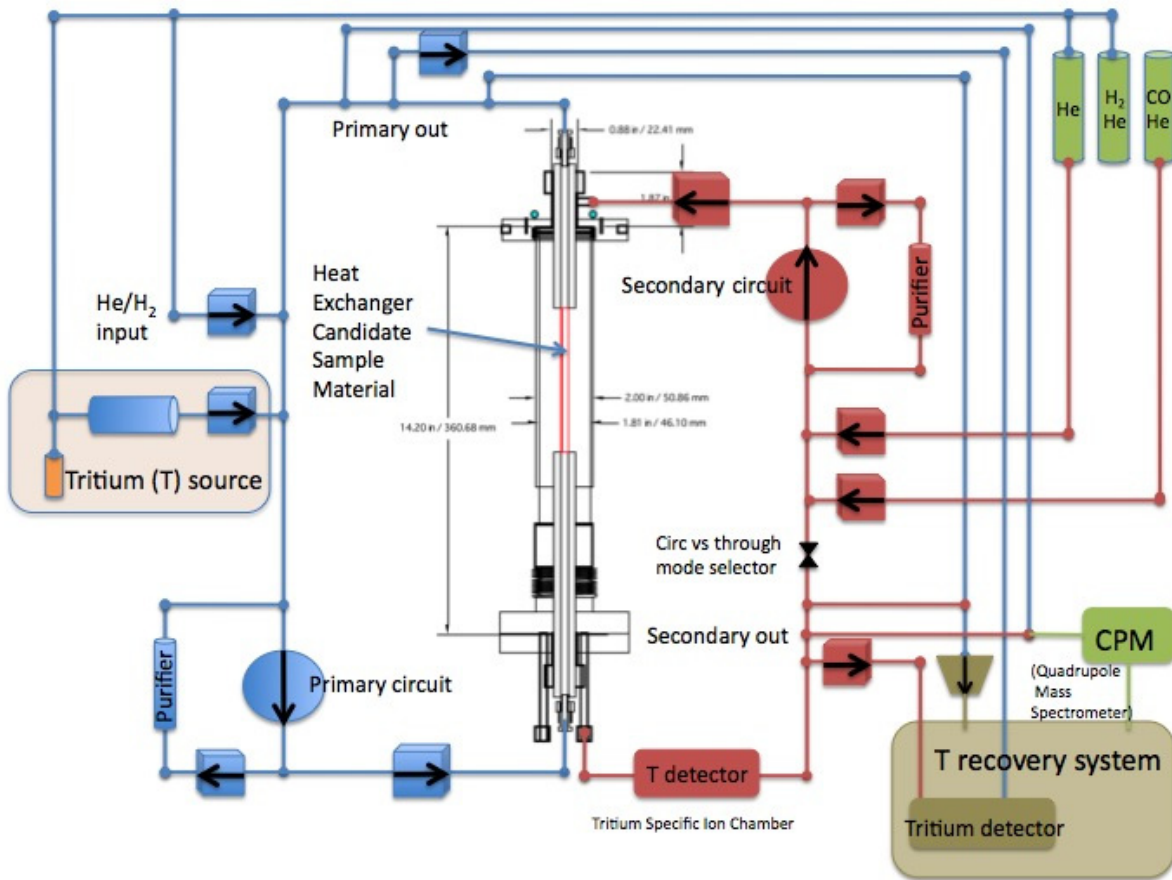
Figure 2(a). Simplified diagram of the permeability measurement system.
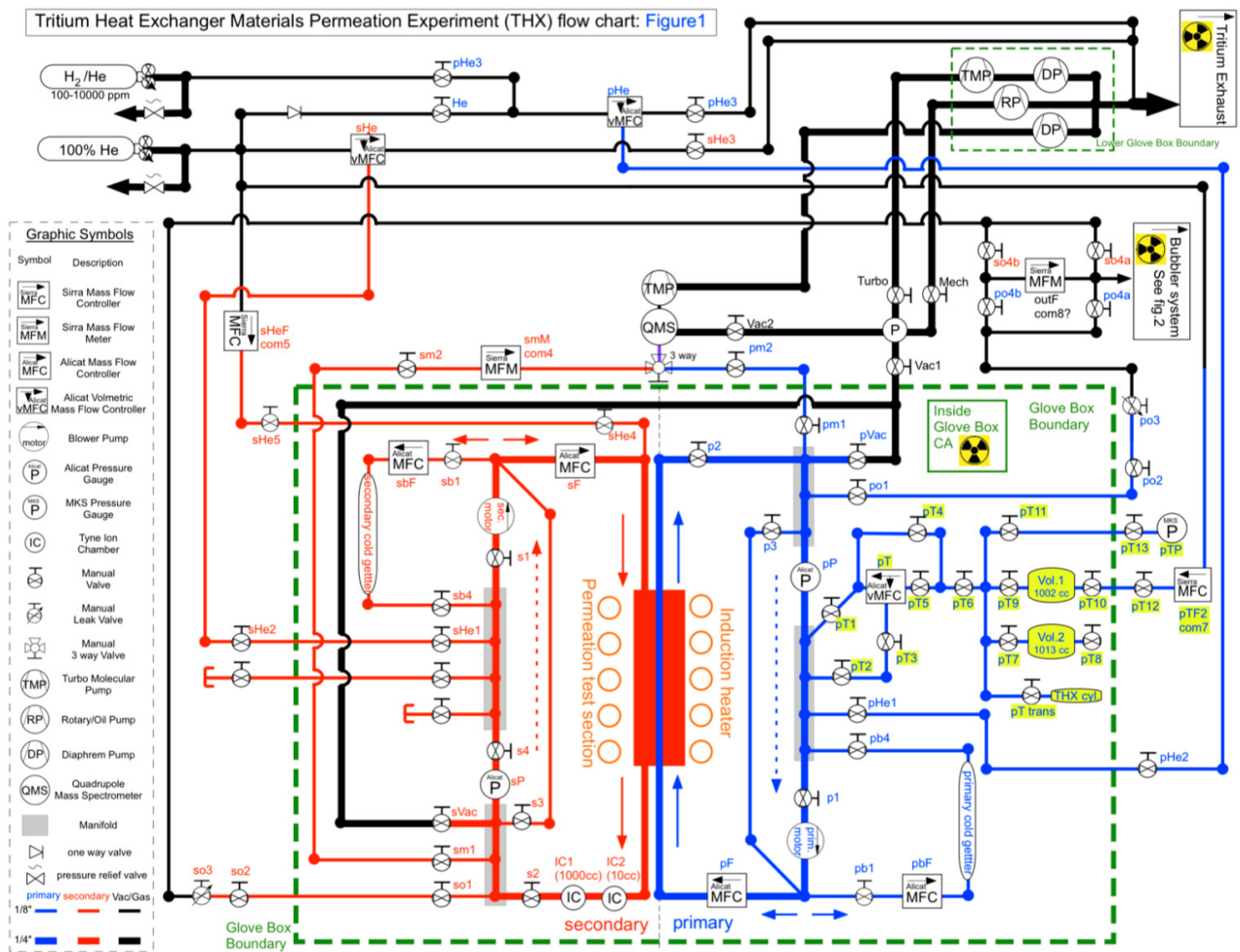
Figure 2(b). Detailed diagram of the permeability measurement system inside the glove box.
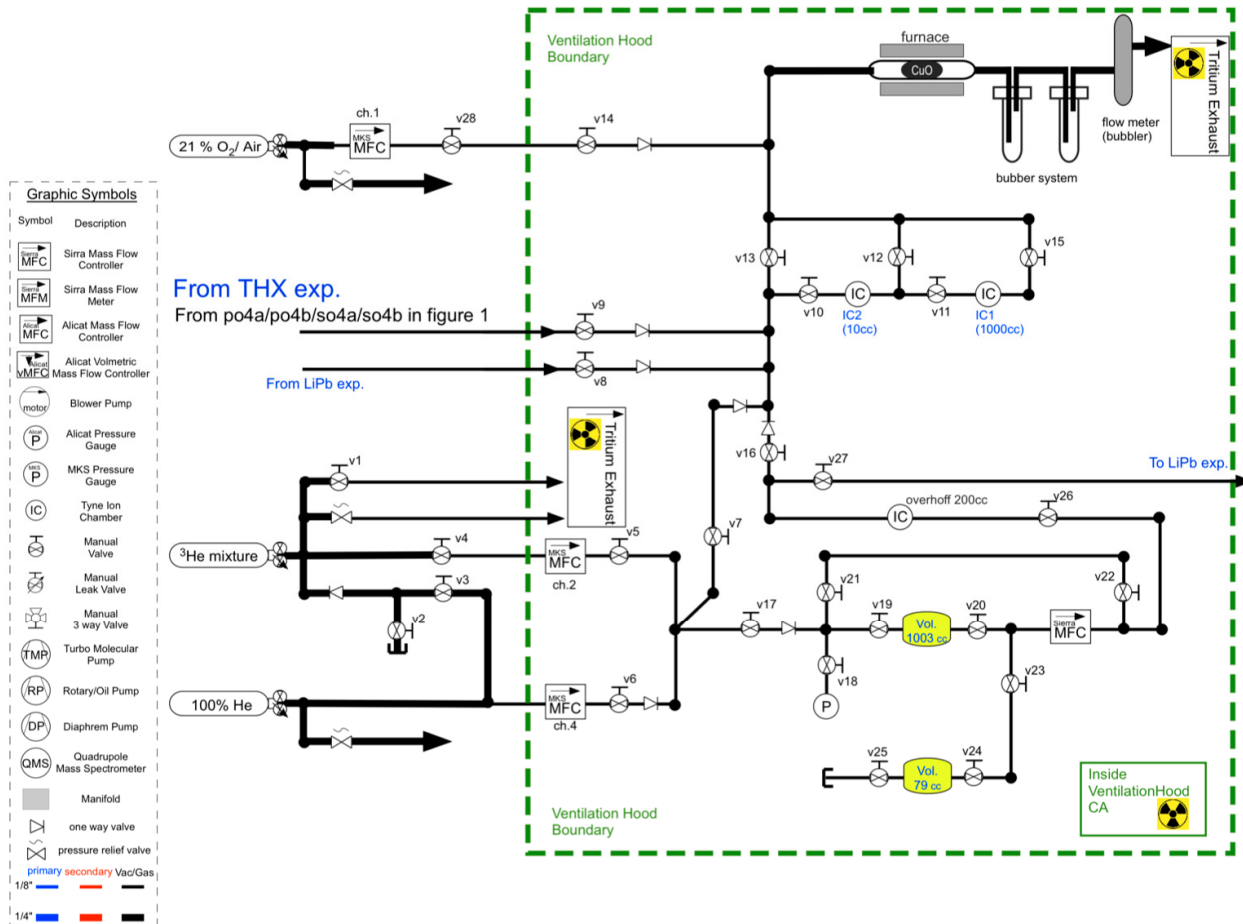
Figure 2(c). Detailed diagram of the permeability measurement system inside the ventilation hood

The permeation measurement system is a sealed system housed in a glove box, as shown in Figure 3, for tritium control in planned tritium testing. The system was fabricated with 316 and 304 stainless steel components, tubing, and welded compression fittings (component sources for the measurement system are listed in Table 2) for vacuum integrity. During the assembly and initial performance testing, the vacuum integrity of the system was established at a leak rate of less than 10^{-5} stdd cc/sec by helium leak testing with mass spectrometry. The system had provisions for introduction of certified hydrogen-helium gas mixtures used for the permeation probe mixture in the primary loop, introduction of ultra-high purity helium for the sweep gas in the secondary loop, getter modules for purification of the helium gas streams, a rotary pump and turbomolecular vacuum pump for evacuation and clean up of the gas loops, and metal bellows pumps for the circulation of the gas flows in the loops.
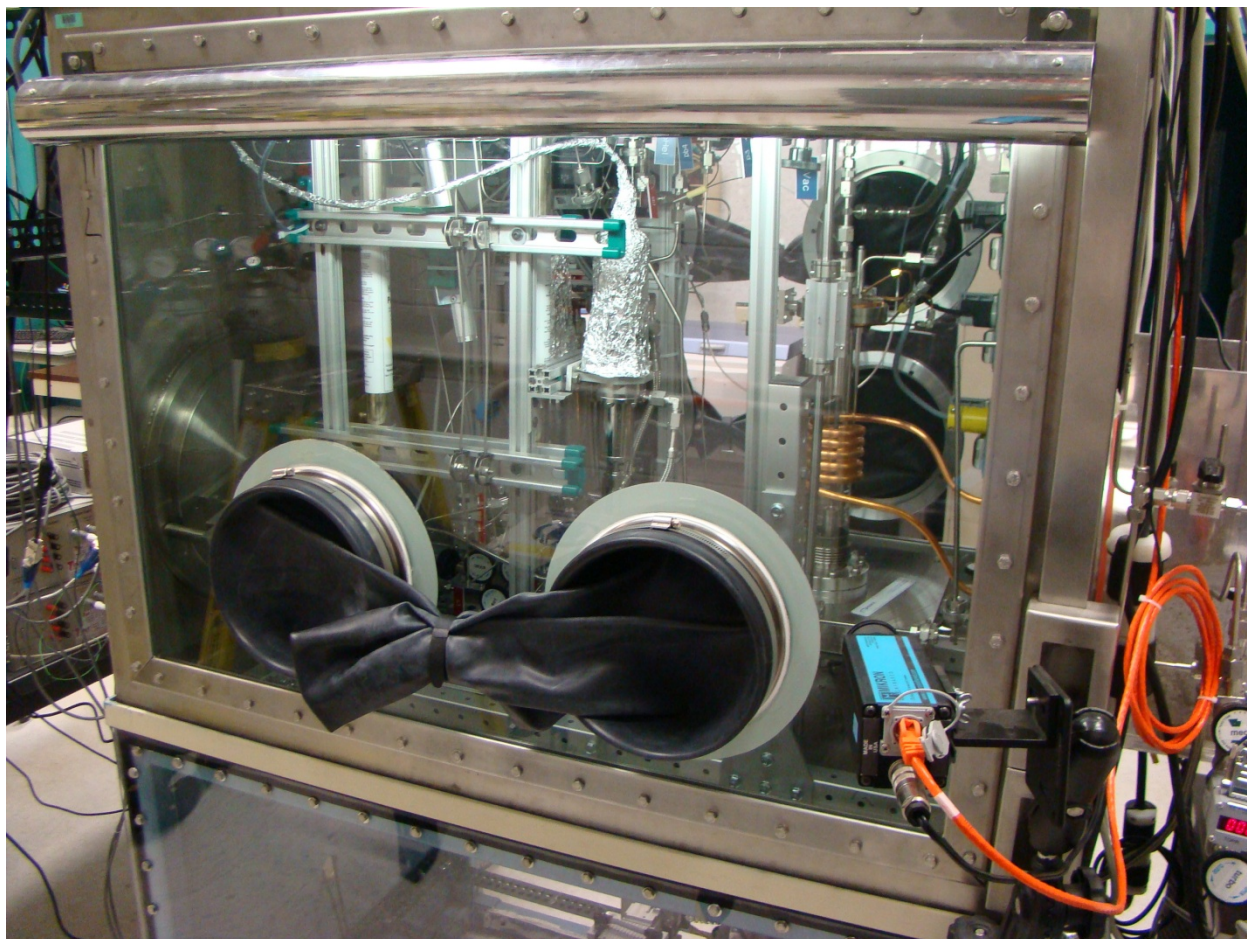
Figure 3. The permeability measurement system assembled within a glove box for work with tritium permeation. Infrared camera is visible connected to orange cable.

Table 2. Sources of components.

Component	Item	Model	Manufacturer
Compression fittings		VCR	Swagelok, Inc.
Purification getters		HP-2, P100-2	VICI Valco Instruments Company, Inc
Rotary pump		RV5	Edwards, Inc.
Turbomolecular pump		TMH 071P	Pfeiffer Vacuum, Inc.
Metal bellows pumps		Model MB-158	Senior Operations, Inc.
Pressure controller	transducer	PCD-30PSIA-D-25VCRM/5P	Alicat Scientific, Inc.
	software	Flow Vision™ SC	Alicat Scientific, Inc.
Mass flow controllers	transducer	MC-10SLPM-D-30PSIA-25VCRM	Alicat Scientific, Inc.
	software	Flow Vision™ SC	Alicat Scientific, Inc.
	transducer	C-100L-DD-8-OV1-PV2-V1-SI-CN	Sierra Instruments, Inc.

Component	Item	Model	Manufacturer
	software	Smart-Trak 2™	Sierra Instruments, Inc.
Process control software		LabVIEW, Version 8.5.1	National Instruments, Inc.
Mass spectrometer	spectrometer	Transpector CPM Compact Process Monitor	Inficon, Inc.
	software	TWare32™	Inficon, Inc.
Sample chamber			Larsen Glass, Inc.
Induction heater		SI-10KWHF	Superior Induction Co.
Control thermocouple	Type K thermocouple		Omega, Inc.
	Read out unit	SXCI-1000	National Instruments, Inc.
Thermal imaging system	infrared camera	M9200	Mikron Infrared, Inc.
	software	MikroSpec R/T™ 9200, Version 3.9200.117	Mikron Infrared, Inc.
Alloys for samples	Incoloy 800H, Inconel 617, and Haynes 230		Century Tubes, Inc.
Sample supports	Inconel 600 tubes		TW Metals, Inc.
Gas mixtures	Nominal 1.5, 3, and 6 ppmv tritium in He		Norco, Inc.
Tritium ion chamber detector	Multi Range Tritium Controller	7000-TC-002-C	Tyne Engineering Inc.
Ion chamber calibration hardware and software for response testing of 10 cc and 1000 cc ion chambers	7500-MKIT-001-C software, Calibration Procedure, Calibrated voltage-current simulator with certification, Calibrated DMM with certification	Calibration Kit 7000	Tyne Engineering, Inc.

The system is instrumented with pressure and mass flow controllers for accurate control of the gas pressure and flow rate. The pressure and mass flow controllers are controlled through a LabVIEW process control software interface. The activity of the input gas mixtures (1.5, 3, and 6 ppm tritium in helium) in the primary loop was measured using the Tyne ion chamber unit located in the tritium recovery hood adjacent to the permeation system glovebox. The output gas in the secondary loop was measured by the Tyne ion chamber unit mounted in the glovebox. The flow composition can alternately be measured using the in-line quadrupole mass spectrometer (CPM), which is capable of sampling gas streams at 1 atm pressure. Because the CPM is mounted outside the glovebox, it is not preferable to run a tritiated gas flow through it. The tritium (and potential hydrogen) gas concentrations are expected to be below its 20 ppm detection limit, and as such little value may be obtained from monitoring with the CPM.

Detection of tritium diffusing into the secondary chamber is done using a Tyne Engineering Model 7000-TC-002-C ion chamber system that is designed explicitly for detection of tritium. This is

multi-range system with 2 ion chambers in series, one with a 10 cc volume, and the other with a 1000 cc volume. The small chamber provides a rapid response, while the larger chamber gives a high sensitivity for low concentrations.

The sample chamber consists of a quartz tube sealed to Kovar transitions between two vacuum flanges, as shown in Figures 2 and 4. The test sample is mounted in the upper and lower vacuum flange by compression O-ring seals, and is terminated with VCR gas compression fittings for connection to the primary loop. In this design, the two helium loops sweep the sample chamber in counter-flow manner, with the tritium-helium probe gas mixture passing upwards through the bore of the tubular sample, and the helium sweep flow of the secondary loop sweeping the external surface of the tubular sample, flowing downward through the main chamber volume.
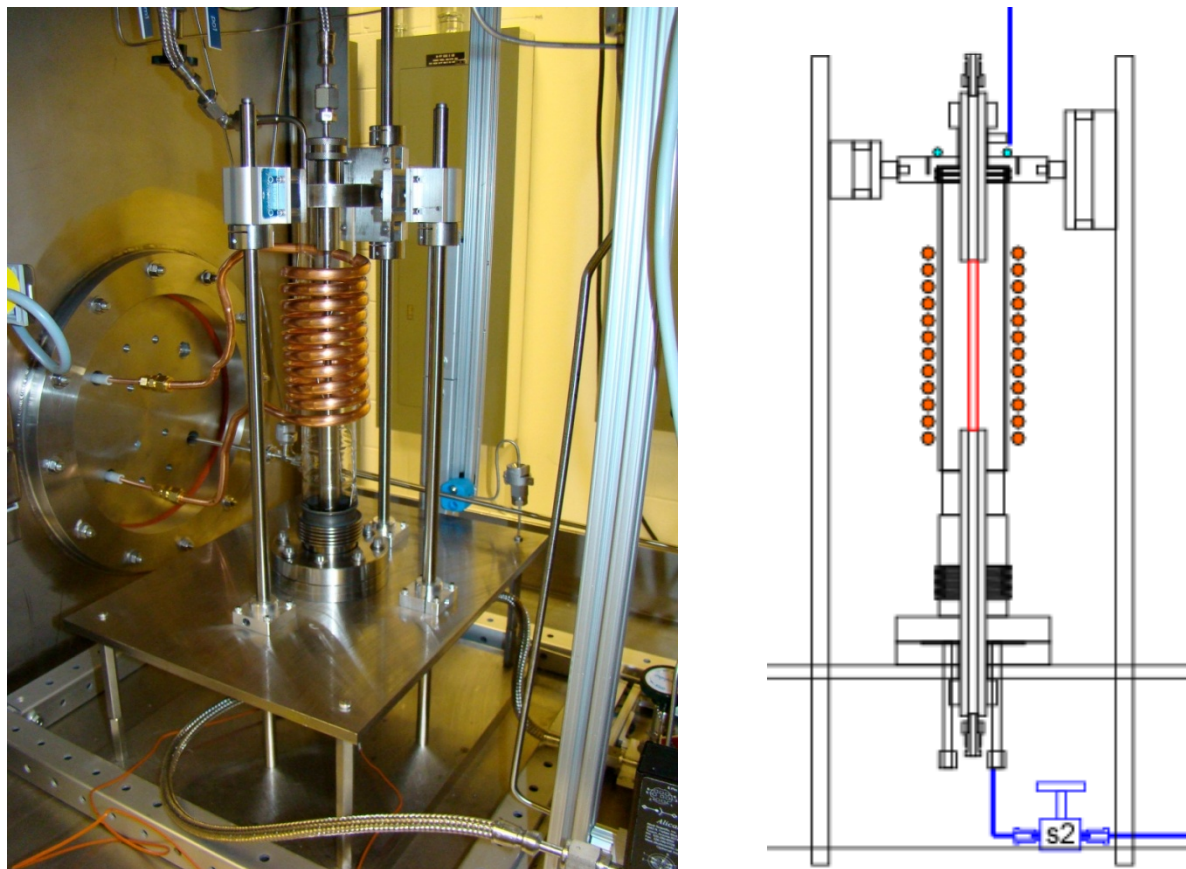
Figure 4. Configuration of the test sample. The picture and drawing show the configuration of the test sample within the quartz-walled test chamber, surrounded by the induction heater coils.

The test sample is heated by a radio frequency induction heater, the copper coils external to the quartz chamber, as shown in Figure 4. The induction heater is a water-cooled, 440 VAC, 100 to 300 kHz, 10 kilowatt system. The induction heater is controlled by the National Instruments LabVIEW process control software interface, using a contact thermocouple that is located at the center (midplane) of the heated area of the test sample.

The temperature of the heated area of the test sample is monitored by an infrared thermal imaging system mounted external to the glove box. The system yields two-dimensional maps of the temperatures of the heated sample area visible in the gaps between the radio frequency heater coils. The system has

four temperatures ranges that span 600 to 1600°C, with spectral response from 800 to 900 nanometers and temperature resolution 0.5% of reading. The thermal imaging system is calibrated against the control thermocouple, allowing evaluation of the emissivity of the sample. Figure 5 shows five regions of interest (oblong boxes) that correspond to the heated Inconel 617 sample visible between the induction coil windings, two lines along which the continuous temperature distribution is recorded, and a tabulation of minimum, maximum, and average temperatures for each region or line of interest.

	Min. °C	Max. °C	Avg. °C	Range °C
Rectangle 1	810.1	861.5	839.1	51.4
Rectangle 2	889.0	914.0	902.2	25.0
Rectangle 3	887.3	912.2	900.2	24.9
Rectangle 4	826.3	862.6	846.9	36.3
Rectangle 5	UNDER	769.0	735.6	
Line 6	UNDER	909.7	UNDER	
Line 7	UNDER	911.1	703.0	
Rectangle 8	UNDER	741.0	UNDER	
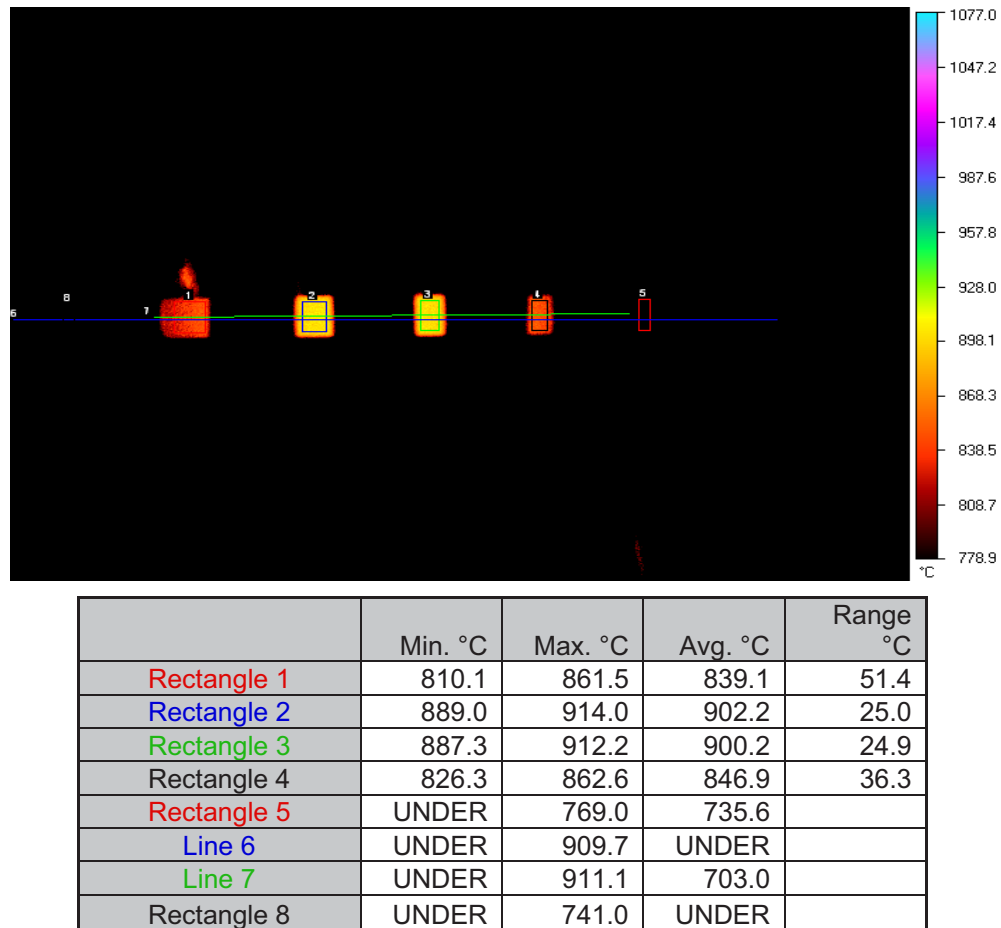
Figure 5. Sample output of the thermal imaging system.

Data along Line 6 is used to fit a continuous temperature distribution that is used in the data analysis. The analytical solution for 1D heat conduction with fixed end temperatures and constant heat generation is quadratic; the data were well fit with this form. The measured and fitted temperature profiles for Incoloy 800H are shown in Figure 6, and for Inconel 617 in Figure 7.
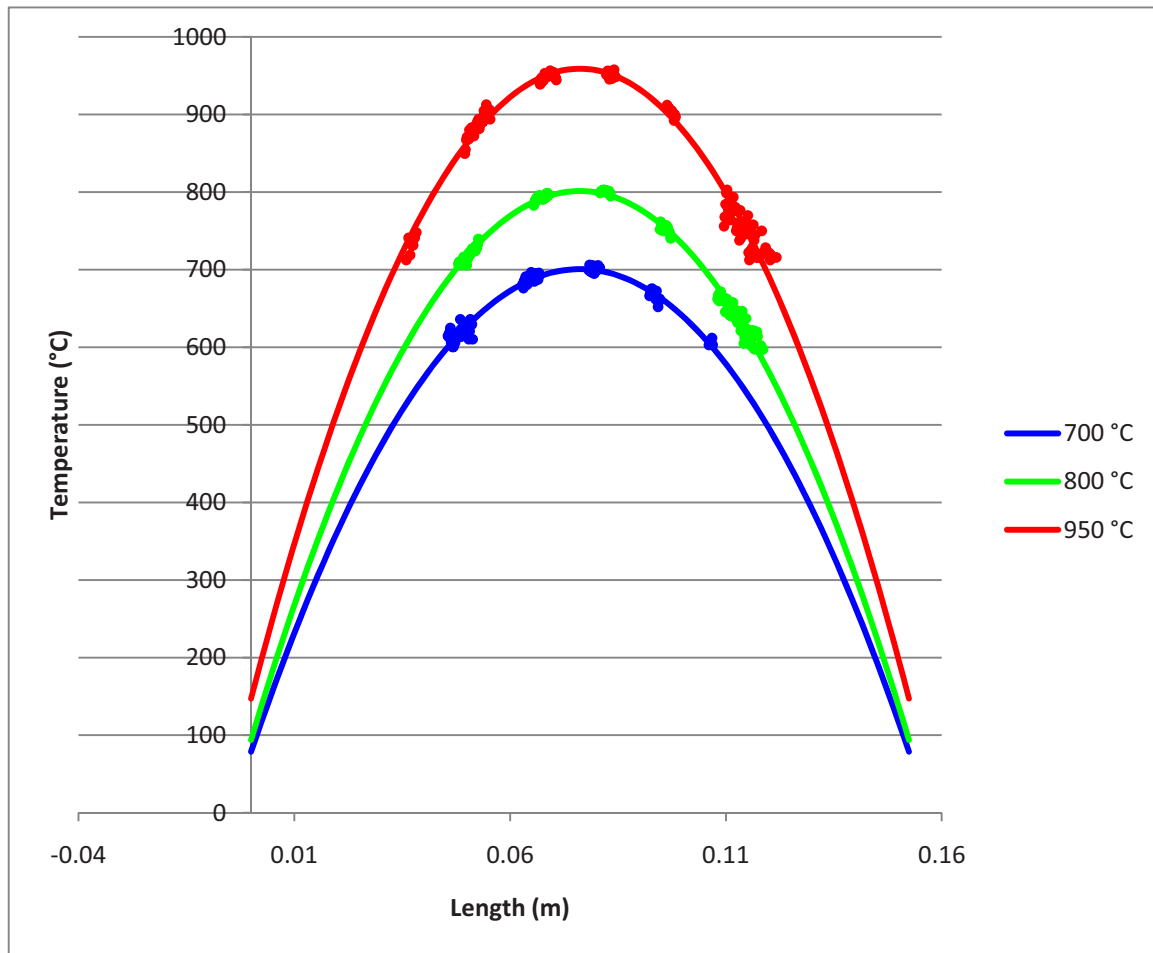
Figure 6. Incoloy 800H axial temperature distribution data and quadratic fit.
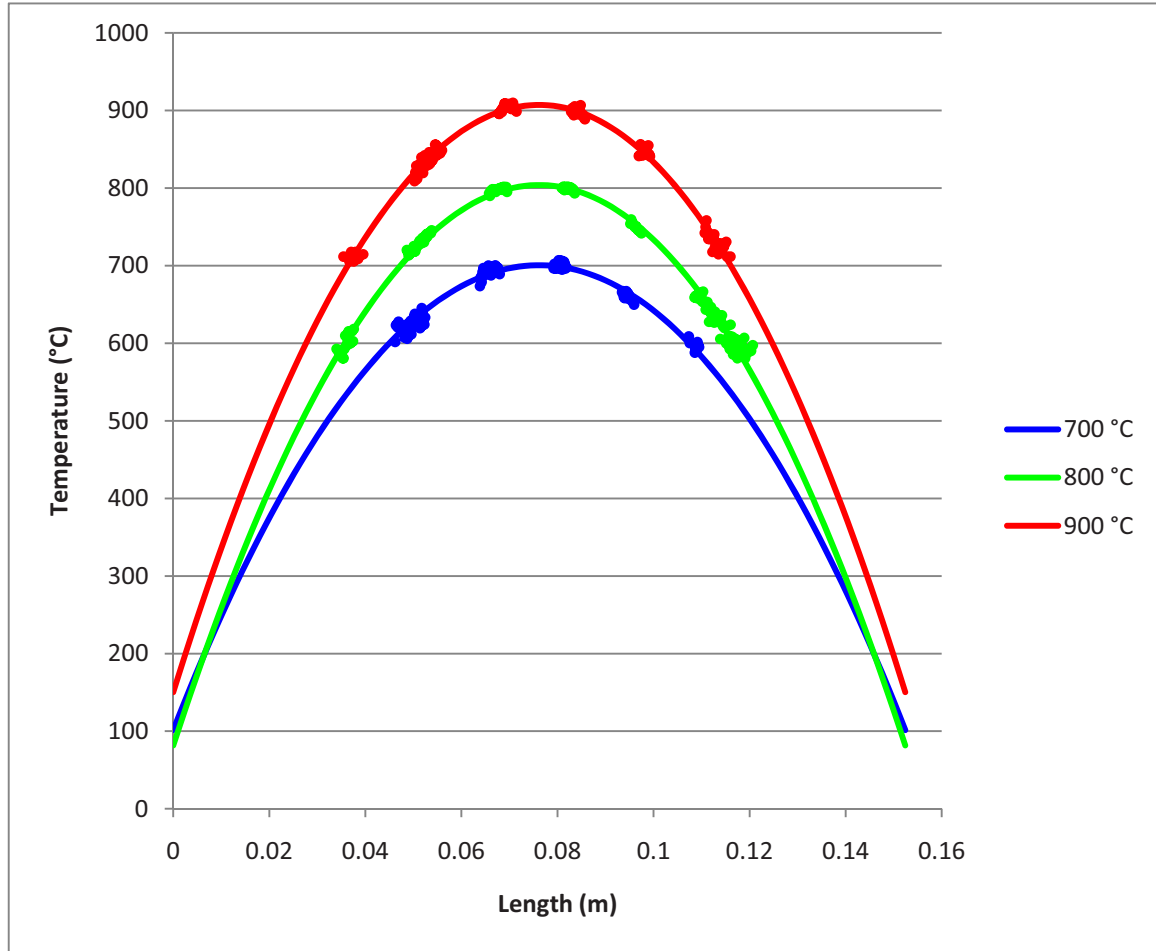
Figure 7. Incoloy 800H axial temperature distribution data and quadratic fit.

3.2   Test Samples

The alloys tested for hydrogen isotope permeability were Incoloy 800H and Inconel 617. The composition of the alloy heats is given in Table 3. These alloys were obtained as thin-walled tubing stock from Century Tubes, Inc., and were used without further preparation other than the machining and cleaning required for welding into the sample configuration.

Table 3. Composition of the alloys used in permeation tests.

Composition	Heat No.	Fe	Ni	Cr	Co	Mo	W	C	Al	
Incoloy 800H, 0.01 in. wall	V01283	46.65	30.84	19.76				0.06	0.37	Ti: 0.48, Si:0.49 Mn: 1.14, Cu: 0.07
Inconel 617, 0.01 in. wall	XX58A7UK	1.55	53.02	22.21	12.46	8.97		0.08	1.04	Ti: 0.29, Si:0.17 Mn: 0.07, Cu: 0.14

The samples tested had nominal 0.010 in. (0.254 mm) wall thicknesses. The diameter of the tube stock is 0.25 in. (6.35 mm). The actual wall thickness was determined by scanning electron microscopy (SEM) of radially sectioned and polished samples. The measured wall thickness for the samples is summarized in Table 4.

13

Table 4. Measured wall thickness of the as-received alloy tube stock.

Alloy	Wall Thickness (mm)		
	Nominal	**Measured**	**Total Uncertainty(%)**
Incoloy 800H	0.254	0.260	4.75
Inconel 617	0.254	0.257	4.46

The sample configuration is shown in Figure 8, and consists of a 6-in.-long test section of Incoloy 800H, or Inconel 617 tube welded to upper and lower thick-walled barrels of Inconel 600. The Inconel 600 tubes are 0.75 in. (19.1 mm) outer diameter and 0.25 in. (6.35 mm) inner diameter; the tubes were gun-drilled from round bar stock. The center portion of the thin-walled test section is the heated permeation zone. The thickness of the barrels and their location outside the heated zone ensure that they do not contribute measurably to the flux of permeating gas. The thick-walled barrel sections of the test sample are sealed by compression O-ring seals to the upper and lower mounting flange of the sample chamber.
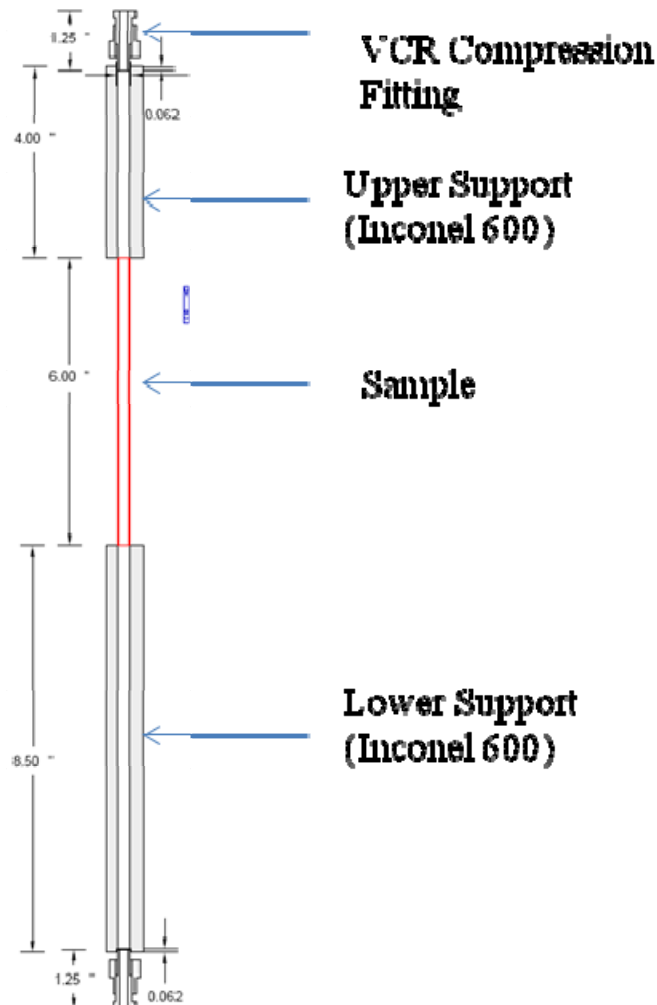
Figure 8. Configuration of the test sample.

The chemical and physical characteristics of the sample materials are described in detail in the hydrogen permeation study published at the end of last fiscal year.[11]

3.3 Gas Mixtures

Preparing tritium/helium gas mixtures is a two step process. The first step utilizes the Tritium Storage and Assay System (SAS) to fill an 11 cc cylinder with a known quantity of tritium. The 11 cc tritium cylinder is then removed from the SAS and connected to the permeation measurement system. The second step involves expanding the tritium into an evacuated volume and then back filling the volume with ultra high purity (UHP) helium to obtain the desired tritium concentrations.

The Tritium SAS provided tritium for these experiments. Tritium is stored in the SAS on two 47 g depleted uranium (DU) beds, each capable of holding 17000 Ci of tritium. At room temperature, a DU bed acts as a vacuum pump that getters all of the hydrogen isotopes. As the temperature of the DU bed is increased, the tritium partial pressure increases as a function of temperature and tritium is released from the DU bed. The SAS relies on pressure-volume-temperature (PVT) measurements and a high purity tritium inventory to determine the quantity of tritium transferred to experiments. The following controls were used to ensure that the SAS accurately measures the quantity of tritium transferred:

W-1.   The accuracy of the pressure sensors are verified annually against manometers whose calibrations are traceable to National Institute for Standards and Technology (NIST) criteria.

W-2.   Volumes were calibrated by filling a reference volume to a known pressure and then expanding the gas into an unknown volume at constant temperature. At least five repetitions of the expansion tests were conducted. Standard data reduction and analysis methods were used to determine the uncertainty associated with each volume. The reference volumes were certified by the Primary Standards Laboratory located at Sandia National Laboratories.

W-3.   The SAS contains nine omega Type-K thermocouples. For Omega Type-K thermocouples above 0ºC the limit of area is 2.2ºC or 0.75% (whichever is greater).

W-4.   Only high purity tritium shipments are received into the SAS and DU bed to DU bed transfers are used to maintain the purity of the tritium inventory by removing ^{3}He decay products.

All tritium transfers are based on the ideal gas law and calculated using:

$$A = (58023 \cdot X_T \cdot P \cdot V)/(R \cdot T),$$

where A (Ci) is the total activity, T_2 gas contains 58023 Ci/mole, X_T is the tritium concentration ($X_T = 1$ following DU bed to DU bed transfers), and P (torr) is the pressure in volume V (cc) at temperature T (K). R (62396 cc·torr/mole·K) is the universal gas constant.

The SAS provided 249 mCi of tritium in an 11.33 cc transfer volume for the Incoloy 800H permeation experiments and 250 mCi of tritium in an 11.35 cc transfer volume for the Inconel 617 permeation experiments.

Mixing the SAS supplied tritium with UHP helium to obtain the desired tritium concentrations takes place in a mixing manifold attached to the permeation measurement system. Components of the mixing manifold include two 1 liter calibrated cylinders, a vacuum pump system, a 5000 torr pressure sensor, a UHP helium supply gas cylinder, a mass flow controller, manual isolation valves, and ~ 15 cc of interconnecting tubing. The 11 cc tritium transfer volume is attached to the mixing manifold with a VCR coupling. The following steps were followed to prepare tritium/helium gas mixtures.

X-1.   Evacuate the entire mixing manifold and then close all of the manual isolation valves.

X-2.   Pressurize one of the 1 liter cylinders to ~4500 torr with UHP helium.

15

X-3.   Expand the tritium in the transfer volume into the 15 cc of evacuated interconnecting tubing. Close the valve on the tritium transfer volume after five minutes.

X-4.   Expand the tritium in the 15 cc of interconnecting tubing into the evacuated 1 liter cylinder.

X-5.   Expand the UHP helium in the 1 liter cylinder into the 15 cc of interconnecting tubing and 1 liter volume containing tritium. Allow the tritium and helium to mix at least overnight to ensure that a relatively consistent tritium concentration is achieved.

The tritium concentration was estimated using PVT calculations and measured with an ion chamber. Due to non-uniform mixing, an estimated concentration was used for determining the operating concentration. This procedure creates a tritium/helium mixture large enough to verify the tritium concentration with an ion chamber and also run three permeation experiments. At the end of the three permeation experiments the mixing manifold was purged with UHP helium and then evacuated. This mixing process was then repeated twice using the tritium remaining in the tritium transfer volume. In this way the primary gas loop of the system was supplied with a tritium/helium mixture at nominal concentrations of 6.0, 3.0, and 1.5 ppm.

Following the mixing process prior to the experiment sequence, the tritium concentration in the primary loop was measured by the ion chamber located in the ventilation hood. The following steps were followed to measure the tritium concentration in the mixture without heating of the test sample:

Y-1.   Pressurized the primary loop to 105 kPa with the T2/He mixture

Y-2.   Turn on the primary motor to circulate the mixture with 1 liter per minute in the primary loop

Y-3.   Open the primary output line and adjust the primary output leak valve to 15 sccm

Y-4.   Measure the tritium concentration in the mixture via the 10 cc ion chamber in the ventilation hood.

Typically three experiments at 700°C, 800°C, and 950°C (900°C for Alloy 617) were performed with one tritium concentration except for one sequence of seven experiments from TS20-1 to TS20-7. Following the experiment sequence, this procedure was repeated to evaluate the tritium concentration in the primary loop. Figure 9 shows the ion chamber response of tritium concentration determination procedure before and after the experiment sequence from TS17-4 through TS17-6. The red line denotes the ion chamber response before the experiment sequence, and the blue line denotes that after the sequence. The t=0 denotes the beginning of the heating. The measured tritium concentrations before and after the experiment sequence are approximately 7.3 and 6.2 Ci/m^3, respectively. This discrepancy in the measured tritium concentration before and after the sequence might be due to the depletion of tritium in the primary loop during the sequence. The measured value before the sequence was used in the analysis in the measurement results section and Table 2.
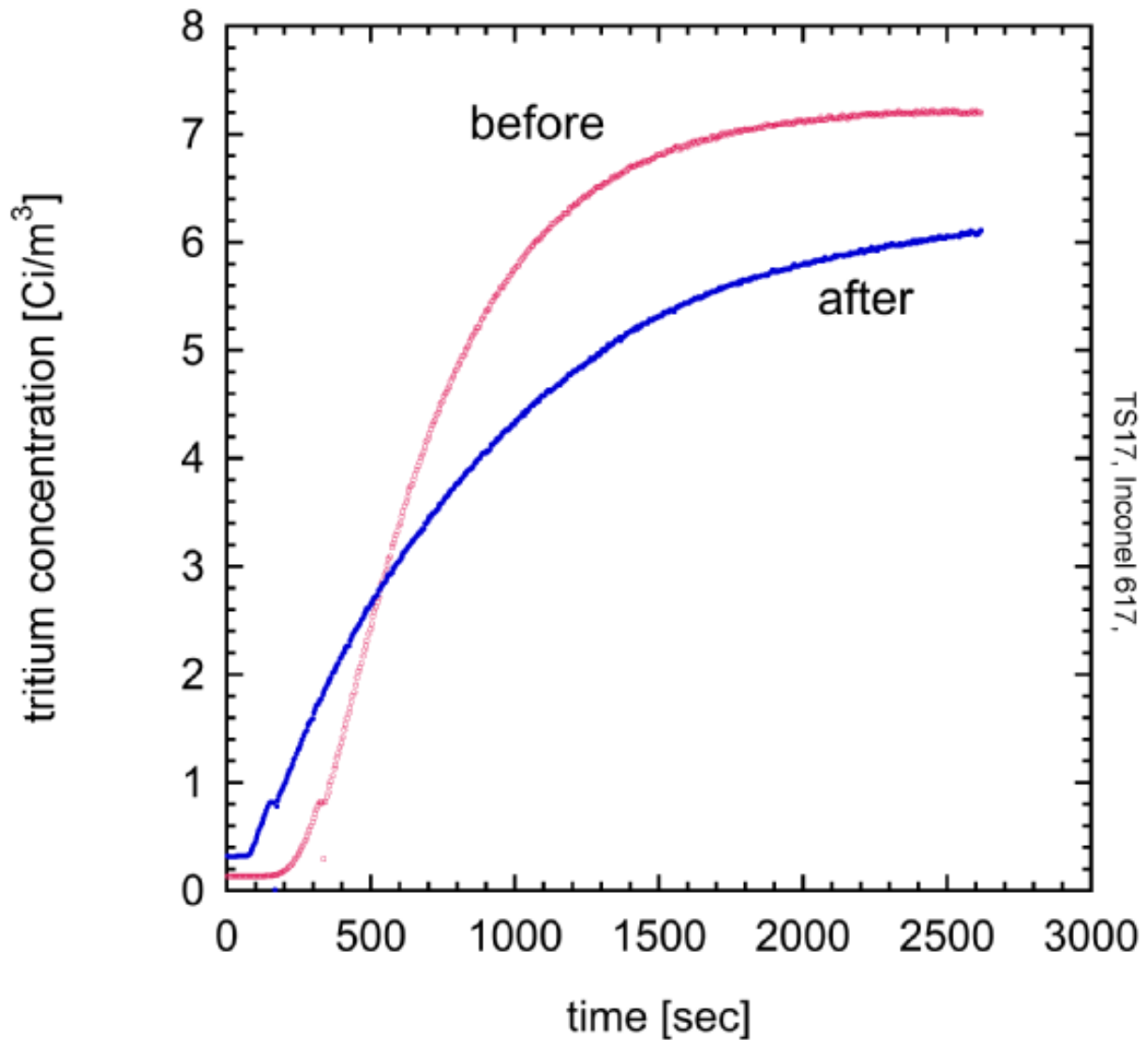
Figure 9. Ion chamber response of tritium concentration determination procedure before and after the experiment sequence from TS17-4 through TS17-6.

Following the tritium concentration determination in the primary loop, the identical procedure was followed for the tritium permeability measurement with the previously reported hydrogen measurement.[11] The only difference in the test procedure is that the two ion chambers were used for the tritium detection instead of the quadrupole mass spectrometer for hydrogen detection.

3.4   Test Parameters

The gas permeability of materials depends on the sample temperature, the wall thickness and heated area of the sample, and the partial pressure of gas constituents on both sides of the sample. Permeability is affected by the oxidation state of the metal surface. The permeability is evaluated by measuring the flux of tritium molecules entering the secondary loop as a function of the total volumetric helium flow rate in the secondary loop and the concentration of hydrogen in the helium flow. The following parameters were measured or controlled during the tests:

- Sample temperature and heated area, including the temperature distribution over the active heated area of the sample

- Concentration of hydrogen in the primary and secondary loops

- Flow rate of helium in secondary loop input line

- Total pressure in primary and secondary loops.

The hydrogen permeability measurements were performed in the recirculation mode of operation. The permeability was measured with hydrogen-helium probe gas mixtures containing nominally 1.5, 3, and 6 ppm tritium in helium at a total pressure of 105 kPa. The measurements were made at sample temperatures of 700°, 800°, and 950°C. The tests were conducted on samples with 0.010 in. (0.254 mm) wall thickness. For Inconel 617, coupling of the radio frequency heater power to the 0.010 in. (2.54 mm) samples was insufficient to heat the 0.010-in.-thick samples above 900°C. Primary loop flow rates ranged from 2 to 15 sccm, and secondary flow was 100 sccm.

4.   MEASUREMENT RESULTS

The permeability tests used tritium in helium in a recirculating mode at primary bleed rates of 2, 6, and 15 sccm. Incoloy 800H and Inconel 617 were tested. In this mode of operation, the tritium in the primary loop can be depleted in modes at low rates of flow. In Figure 10, the blue trace represents the response of the 10 cc ion chamber monitoring the secondary tritium concentration along with the thermocouple temperature response. The red trace is the 1000 cc ion chamber, which has a slower response and a higher sensitivity.
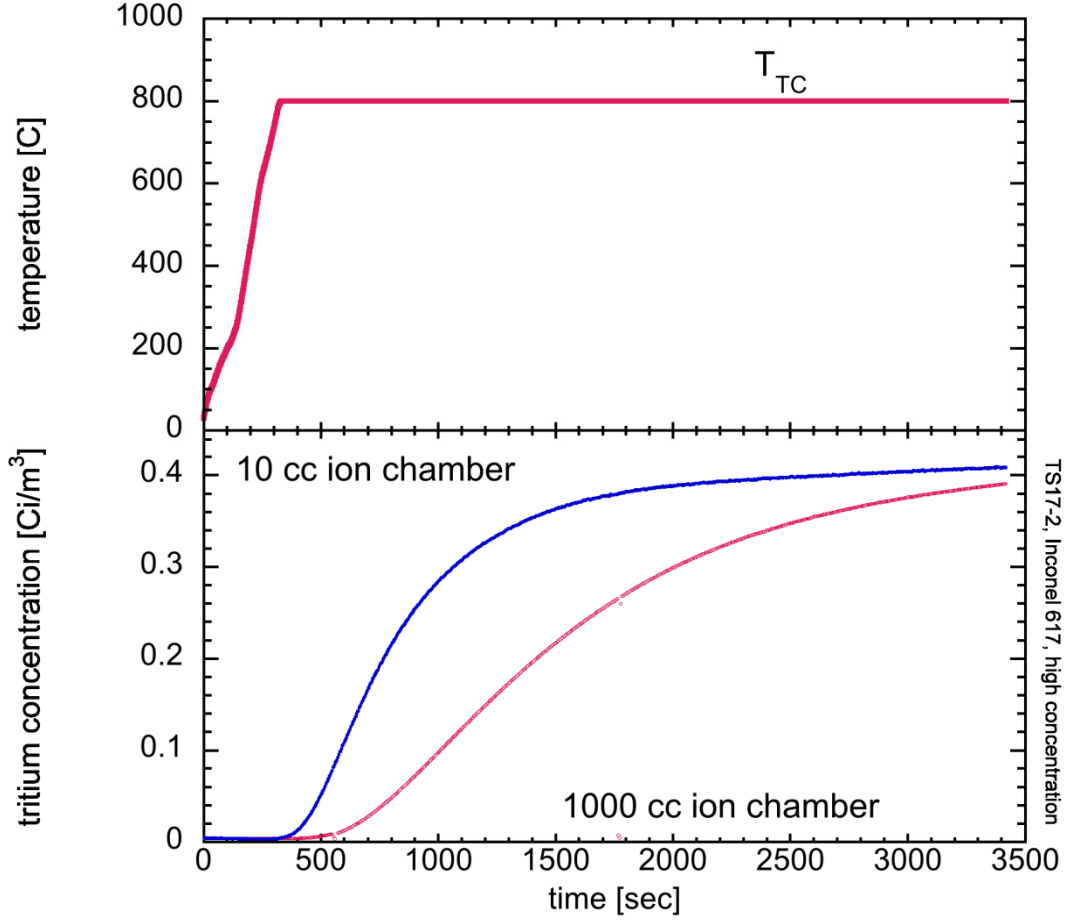
Figure 10. Temperature and Ion Chamber Response Test TS17-2, Alloy 617 at 800°C with gas flow 15 sccm.

Tritium molecules (T_2) present in the primary helium flow will dissociate at solid surfaces and permeate into the solid as individual atoms. The well-known equilibrium relation between T_2 partial pressure in the gas P_{T_2} and the T atom concentration C_T at the interface is Sieverts' law,[15]

$$C_T = S\sqrt{P_{T_2}} \tag{1}$$

where S is the solubility, which has units ($1/m^3 \cdot Pa^{1/2}$) or ($1/cm^3 \cdot atm^{1/2}$). The T atoms in the metal diffuse through it according to Fick's law, which gives the constant flux J

$$J = -D\frac{\partial C_T}{\partial x} = D\frac{C_{T,1} - C_{T,2}}{x} \tag{2}$$

in terms of the primary side (Subscript 1) and secondary side (Subscript 2) T atom concentrations, the wall thickness x, and the diffusion coefficient D. Since Sieverts' law applies at both primary and secondary solid-gas interfaces, Equations 1 and 2 can be combined to obtain the permeation model,[4,5,1210,12,16,17]

$$J_{T_2} = \frac{K\left(\sqrt{P_{T_2,1}} - \sqrt{P_{T_2,2}}\right)}{x} \tag{3}$$

where K is the permeability, the product of solubility and diffusivity (S•D), which has units (mol/m•s•Pa$^{1/2}$) or [(cm^3 T$_2$ @ STP)/(cm•s•atm$^{1/2}$)]. Note the definition of J_{T_2} in terms of molecules, though tritium diffuses as atoms through the solid.

Since clean helium enters the secondary inlet, the tritium mass flow downstream on the secondary side is equal to the tritium mass flow due to permeation through sample:

$$J_{T_2} A = C_{T_2,2} \dot{V}_{He,2} \tag{4}$$

where $C_{T_2,2}$ is the T$_2$ concentration in the secondary flow, $\dot{V}_{He,2}$ is the secondary helium flow rate, and A is the test section area through which permeation occurs. Combining Equations 3 and 4, the following expression for the permeability K is obtained:

$$K = \frac{C_{T_2,2} \dot{V}_{He,2} x}{A\left(\sqrt{P_{T_2,1}} - \sqrt{P_{T_2,2}}\right)} \tag{5}$$

All quantities on the right hand side are known or measured in the experiment, so the permeability can be calculated for each data point with Equation 5.

The permeability K is temperature dependent, and follows an Arrhenius law,

$$K = K_0 \exp\left(\frac{-Q}{RT}\right) \tag{6}$$

where: K_0 is the temperature-independent permeability constant, Q is the activation energy of permeation, R is the universal gas constant, and T is absolute temperature. A plot of the measured permeabilities vs. measured temperatures can be fit by Equation 6 to determine the parameters K_0 and Q. However, this fitting is not straightforward for this particular experiment, because the temperature varied considerably along the test section. Thus, it is not obvious at which temperatures the measured permeabilities should be plotted. In a previous analysis of hydrogen permeation in this experiment, this issue was dealt with by fixing the temperature at the nominal (peak) value, and reducing the sample length (or equivalently, the permeation area) used to calculate permeation (Equation 5). The "reduced length" was based on engineering judgment.

Since the temperature distribution was measured and fit with a quadratic function as discussed in Section 3.1, this function can be used to properly calculate the effective temperature. The full sample length L (6 in. or 15.24 cm) was used to calculate permeability from the experiment data. This permeability represents an average permeability $\bar{K}$ over the length of the sample and its range of

temperatures. Since permeability is a function of temperature, and the temperature is a function of sample length x ($0 \leq x \leq L$),

$$K(x) = K_0 \exp\left(\frac{-Q}{RT(x)}\right) \tag{7}$$

$T(x)$ has the quadratic form

$$T(x) = -Ax^2 + Bx + C \tag{8}$$

and the positive constants A, B, and C are determined from the IR camera data. Then the permeability may be written:

$$K = K_0 \exp\left(\frac{-Q}{R(-Ax^2 + Bx + C)}\right) \tag{9}$$

The average permeability, $\overline{K}$, is simply the integral from $x = 0$ to $x = L$, divided by the total length L:

$$\overline{K} = \frac{1}{L} \int_0^L K_0 \exp\left(\frac{-Q}{R(-Ax^2 + Bx + C)}\right) dx \tag{10}$$

The parameters K_0 and Q are determined by fitting a discretized form of the above integral equation to the measured permeation data with an iterative, non-linear least-squares procedure.[b] The resulting values for both alloys are summarized in Table 5; literature values have been given previously in Table 1. The variation of permeability along the sample length (Equation 9) is shown in Figures 11 and 13, and the Arrhenius plots displaying the experiment data, fit, and literature data are shown in Figures 12 and 14. In the Arrhenius plots, the measured permeabilities $\overline{K}$ from the experiment are plotted at the equivalent temperature $\overline{T}$, defined by

$$\overline{T} = \frac{-Q}{R \ln\left(\frac{\overline{K}}{K_0}\right)} \tag{11}$$

This is the temperature at which the permeability K (given by Equation 6) equals the measured average permeability $\overline{K}$. The same concept has been employed in previous permeation experiments with variable temperatures.[18] A peculiar aspect of Equation 11 is that the plotted *experiment* temperatures depend on the fit parameters; this is an inescapable consequence of making single permeation measurements over a range of temperatures, in which a functional relationship between K and T must be assumed.

The data collected in the permeability tests of both alloys are summarized in Tables A-1 and B-1, and Appendixes A, and B.

---

b. Normally such a procedure would include a weighting of points based on their statistical error; lacking any quantitative information on it here, this weighting was not included.

Table 5. Measured hydrogen permeability values of Incoloy 800H and Inconel 617.

Alloy	K_0 cm^3 (STP)/cm·s·atm$^{1/2}$	Q kcal/mol
Incoloy 800H	1.02e-2	25.1
Inconel 617	1.51e-1	29.8
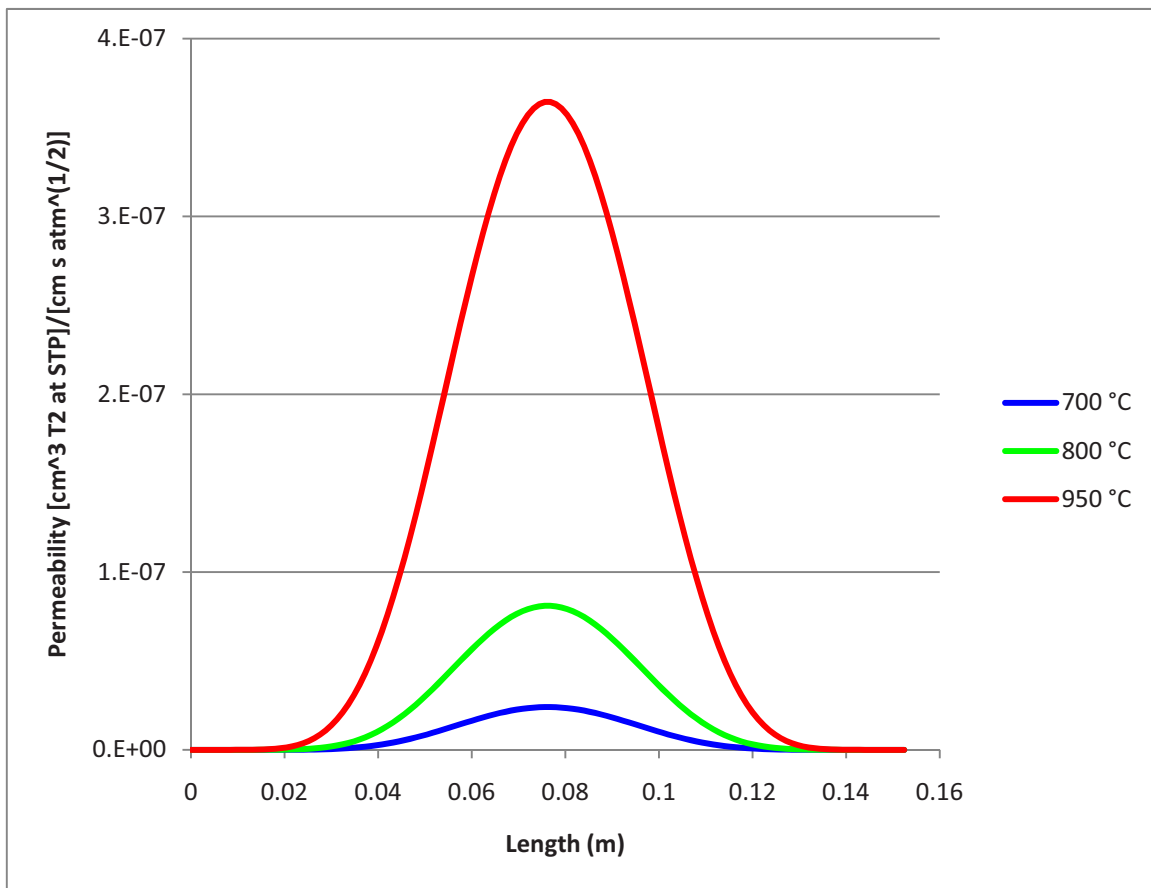
Figure 11. Variation of Incoloy 800H permeability along the sample length.
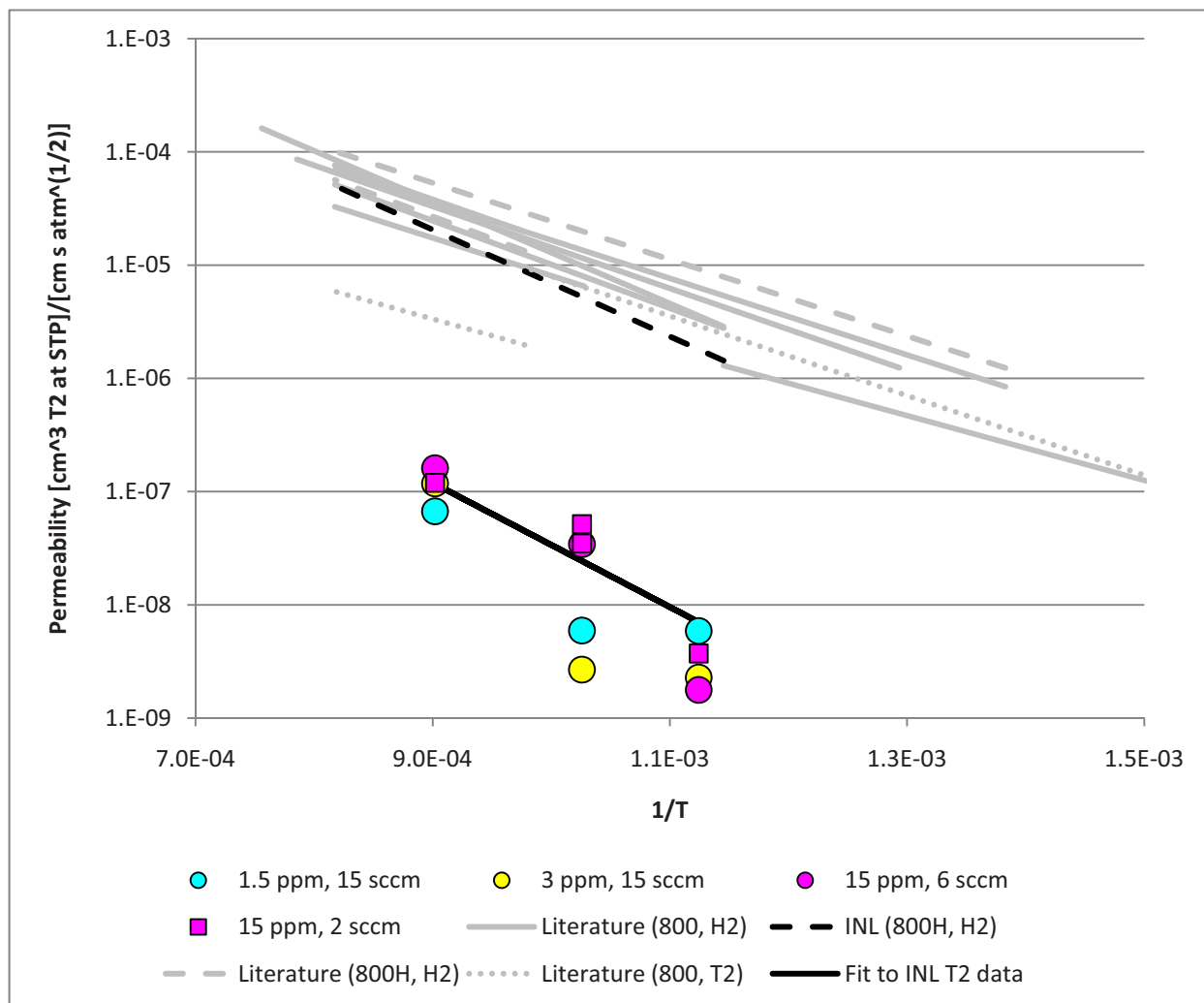
Figure 12. Arrhenius plot of Incoloy 800H tritium permeability with literature data.
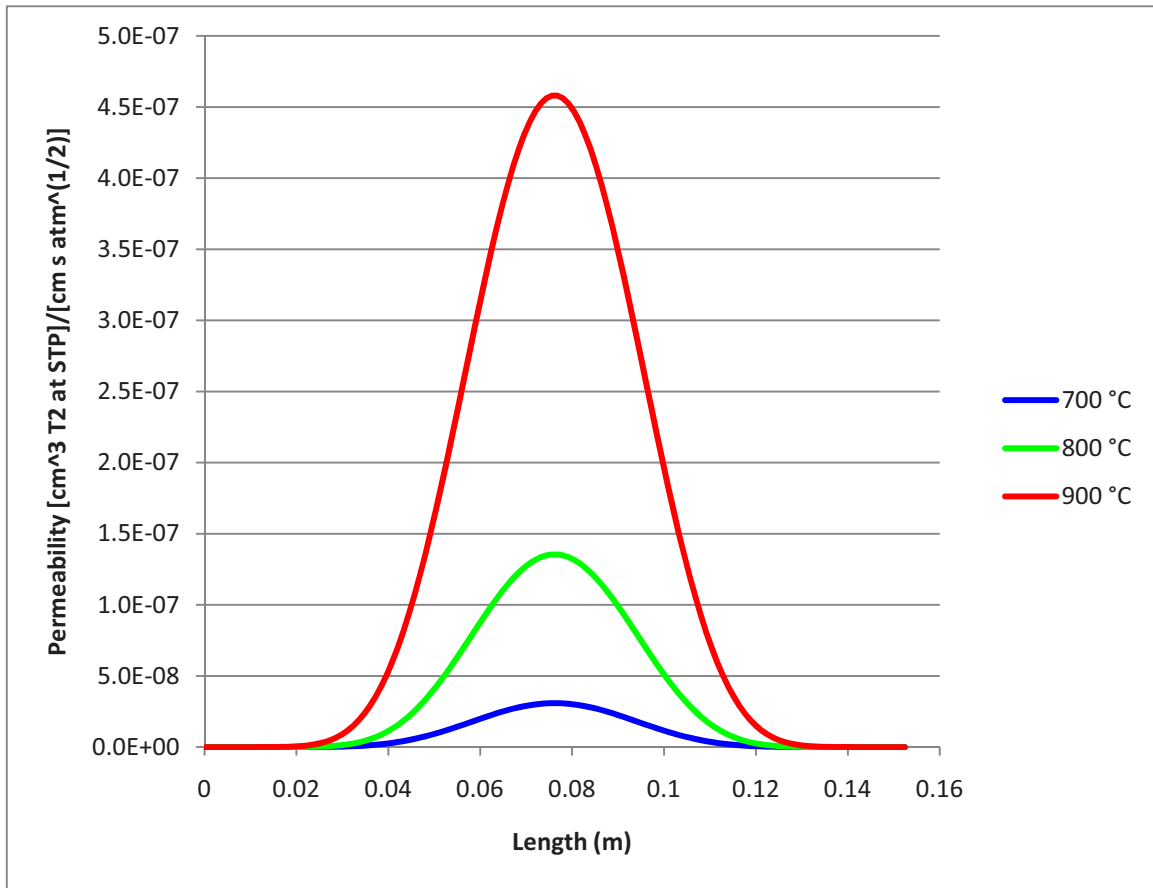
Figure 13. Variation of Inconel 617 permeability along the sample length.
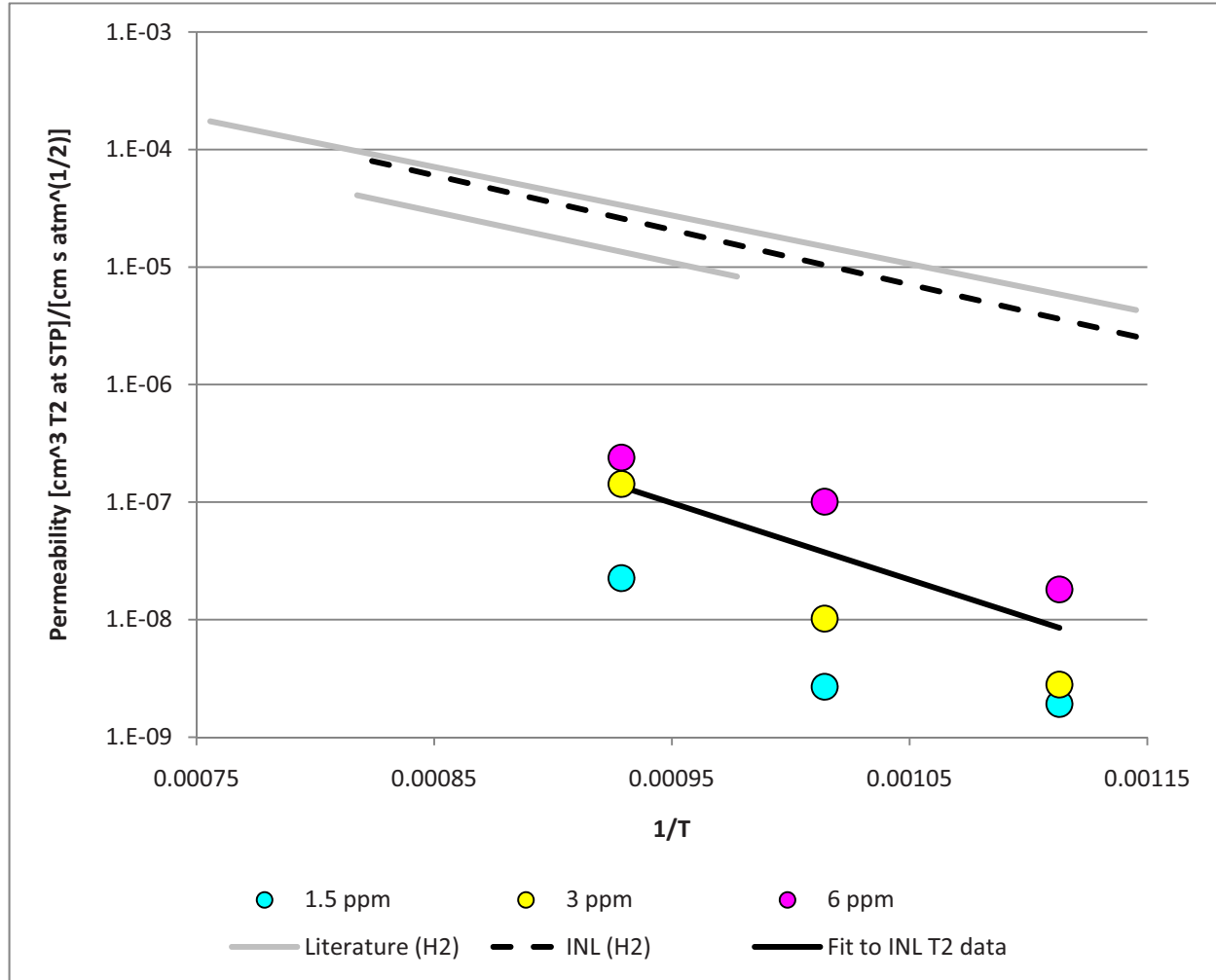
Figure 14. Arrhenius plot of Inconel 617 tritium permeability with literature data.

It is apparent from the figures that for both alloys, the calculated permeability is much lower than has been reported in the literature. A likely reason for this is that in calculating the permeability from the experiment data, it was tacitly assumed that tritium was the only hydrogen isotope present in the system. In reality, prior measurements[11] found a persistent H_2 background of around 16 ppm. Since this is on the on the order of, and in some cases much larger than, the primary T_2 concentration, it needs to be accounted for in the calculation; the dissociation and adsorption/desorption behavior at the surface is a chemical effect, that should not depend on the isotope. In this case, Sieverts' law governs the *combined* pressures and concentrations of all hydrogen isotopes:

$$C_H + C_T = S\sqrt{P_{H_2} + P_{T_2}} \tag{12}$$

Since the T/H ratios should be the same for surface atoms and gaseous molecules,

$$\frac{C_H}{C_T} = \frac{P_{H_2}}{P_{T_2}} \tag{13}$$

Combining Equations 12 and 13 and solving for C_T gives

$$C_T = \frac{SP_{T_2}}{\sqrt{P_{T_2} + P_{H_2}}} \tag{14}$$

Applying Fick's law as in Equations 2 and 3 above, a new expression for the T_2 flux is obtained:

$$J_{T_2} = \frac{K}{x} \left| \frac{P_{T_2,1}}{\sqrt{P_{T_2,1} + P_{H_2,1}}} - \frac{P_{T_2,2}}{\sqrt{P_{T_2,2} + P_{H_2,2}}} \right| \tag{15}$$

Carrying this expression through the same mass balance outlined in Equations 4-5 above, the permeation is given by

$$K = \frac{C_{T_2,2} \dot{V}_{He,2} x}{A \left[\frac{P_{T_2,1}}{\sqrt{P_{T_2,1} + P_{H_2,1}}} - \frac{P_{T_2,2}}{\sqrt{P_{T_2,2} + P_{H_2,2}}} \right]} \tag{16}$$

This method of dealing with mixtures of hydrogen isotopes is widely used in the literature.[19] Note that K in Equation 16 is the *tritium* permeability, and that hydrogen has its own permeability which can be solved for beginning with Equation 12.

In addition to the presence of hydrogen, the calculation is affected by uncertainty in the primary tritium concentration; there was no ion chamber available to measure it during the tests. One of the secondary ion chambers was connected to the primary before each series of tests (fixed concentration at three different temperatures) to measure the initial primary concentration without heating (see Section 3.3), then reconnected to the secondary side for the test series. This measured value was used in the calculation above, and it generally differed significantly from what was calculated for the initial gas mixture. To estimate this effect, the primary concentration was back-calculated from the measured secondary concentration and the value shown by the ion chamber located in the fume hood which measures the combined primary and secondary exhaust. In order to estimate this effect, the primary concentration was back-calculated from the ion chamber connected to the fume hood, through which the combined primary and secondary were exhausted, and the measured secondary concentration. These values were typically lower still than the initial series measurement. The three sets of estimated primary concentrations are shown in Table 6.

Table 6. Primary tritium concentration determined by three different methods: (1) calculated based on the initial gas mixing, (2) measured once prior to each test series and assumed constant for the three temperature measurements in the series; and (3) back-calculated from the fume hood exhaust.

Material	Test ID	Tritium concentration (Ci/m^3)		
		Method 1	Method 2	Method 3
Incoloy 800H	TS20_1	15.39	15.00	9.50
	TS20_2	15.39	15.00	4.99
	TS20_3	15.39	15.00	5.02
	TS20_4	15.39	15.00	5.18
	TS20_5	15.39	15.00	3.61
	TS20_6	15.39	15.00	4.66
	TS20_7	15.39	15.00	4.63
	TS20_8	3.06	7.80	5.97
	TS20_9	3.06	7.80	5.95
	TS20_10	3.06	7.80	4.08
	TS20_11	0.68	4.08	4.26
	TS20_12	0.68	4.08	4.39
	TS20_13	0.68	4.08	3.79
Inconel 617	TS17_1	35.89	15.54	10.04
	T170_2	35.89	15.54	9.57
	TS17_3	35.89	15.54	8.35
	TS17_4	7.46	7.31	5.15
	TS17_5	7.46	7.31	4.69
	TS17_6	7.46	7.31	3.36
	TS17_7	3.06	7.80	4.28
	TS17_8	3.06	7.80	4.24
	TS17_9	3.06	7.80	4.63

If the equations corrected for the presence of hydrogen (at 16 ppm) are used to calculate permeability, and the primary tritium concentrations determined from the hood exhaust are used, the permeability is considerably higher, as shown in Figures 15-18. The fit parameters for this case are given in Table 7.

Table 7. Measured tritium permeability values of Incoloy 800H and Inconel 617 (with hydrogen and detector corrections).

Alloy	K_0 cm^3 (STP)/cm·s·atm$^{1/2}$	Q kcal/mol
Incoloy 800H	1.05e-2	27.1
Inconel 617	6.61	35.6
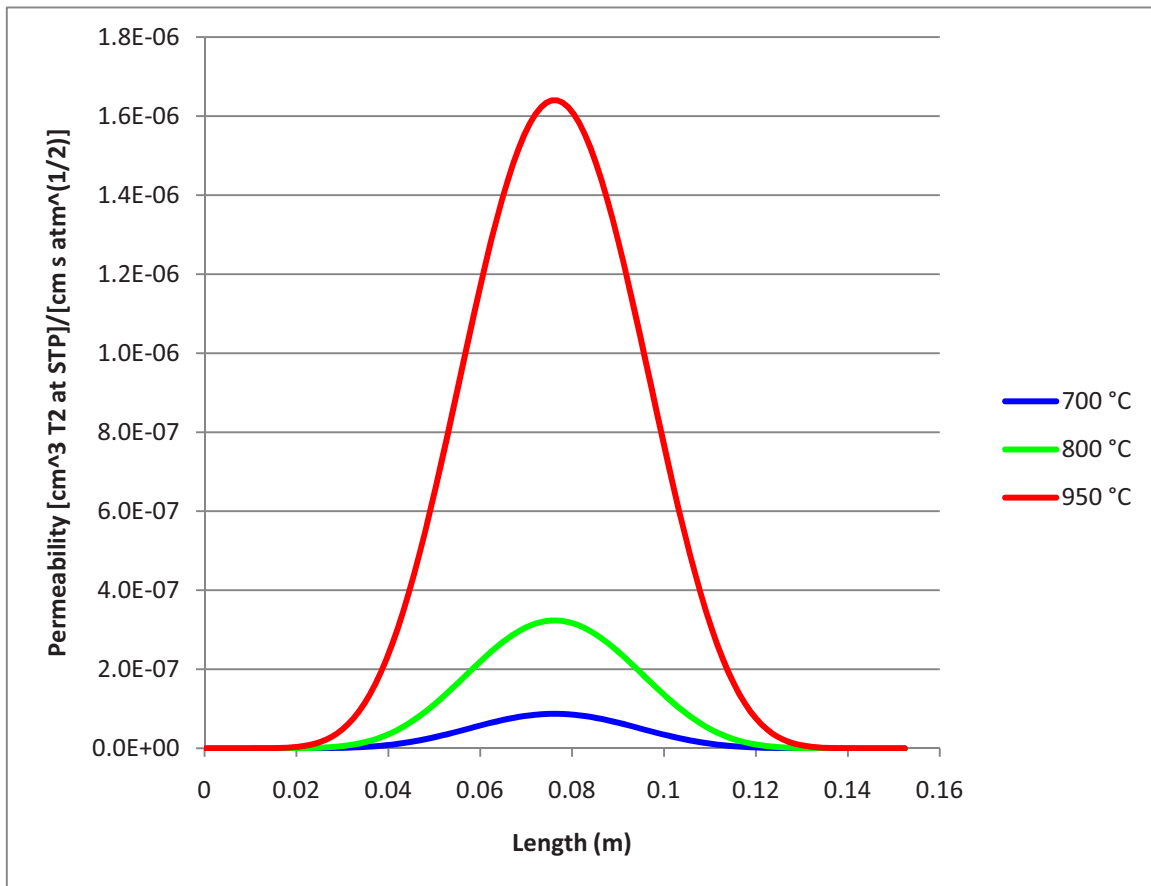
Figure 15. Variation of Incoloy 800H permeability along the sample length (including hydrogen and detector corrections).
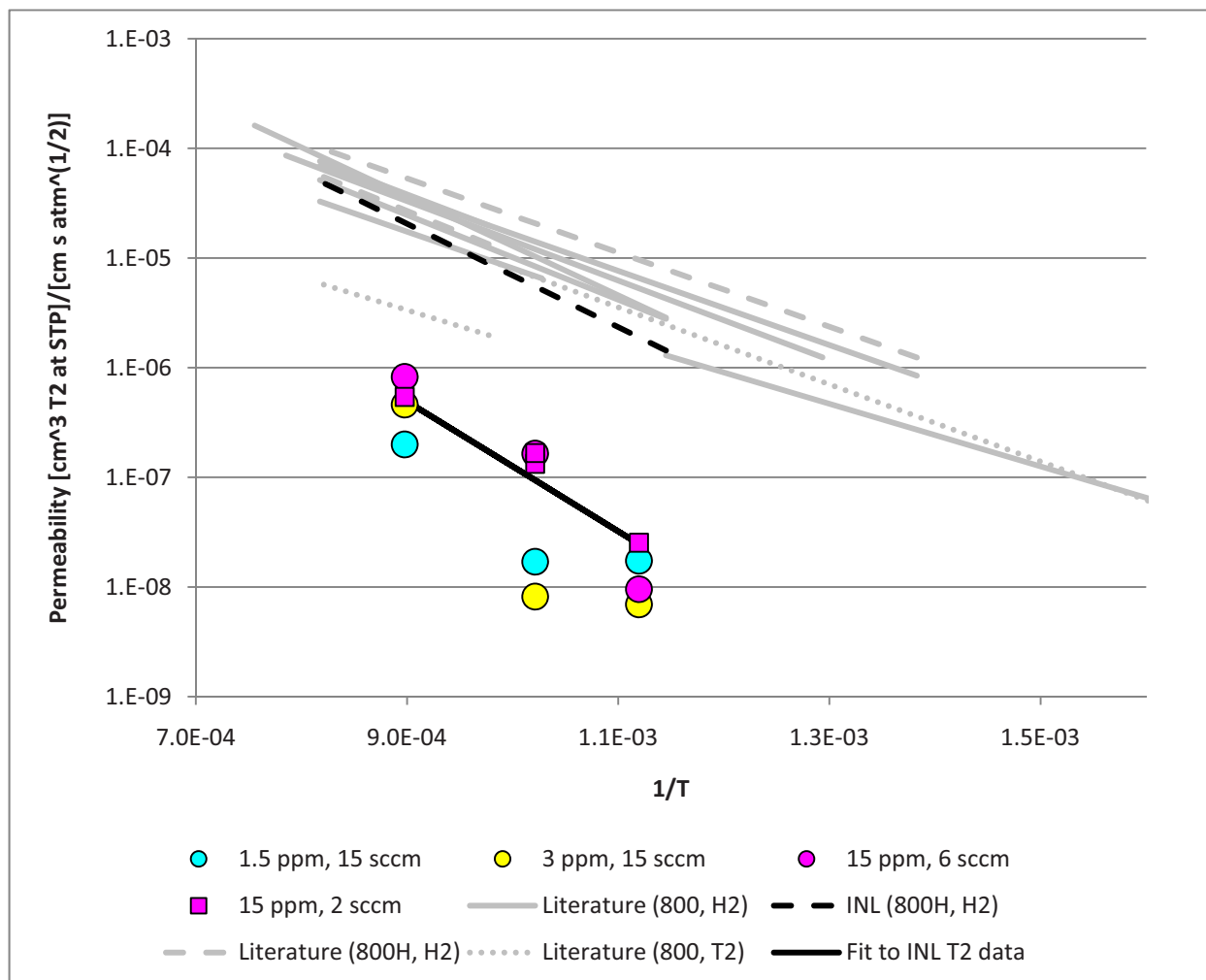
Figure 16. Arrhenius plot of Incoloy 800H tritium permeability with literature data (including hydrogen and detector corrections).
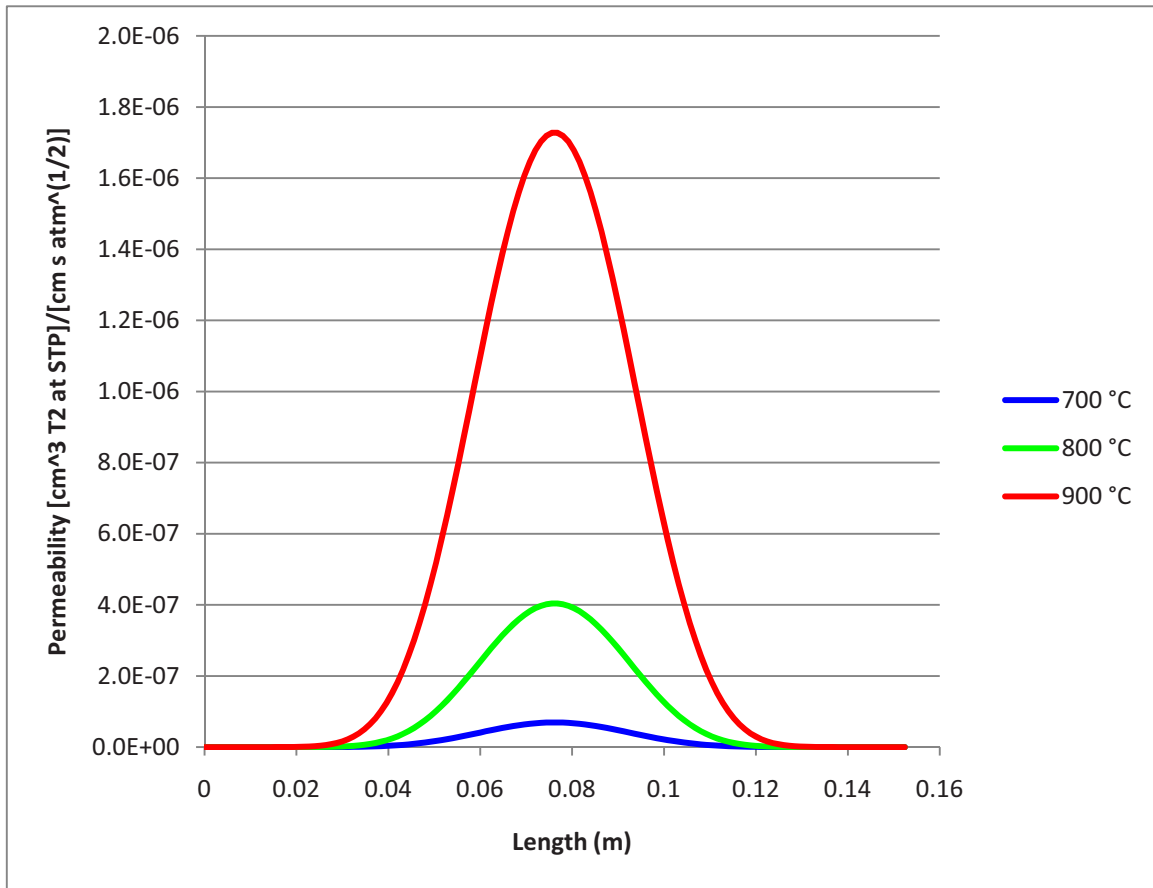
Figure 17. Variation of Inconel 617 permeability along the sample length (including hydrogen and detector corrections).
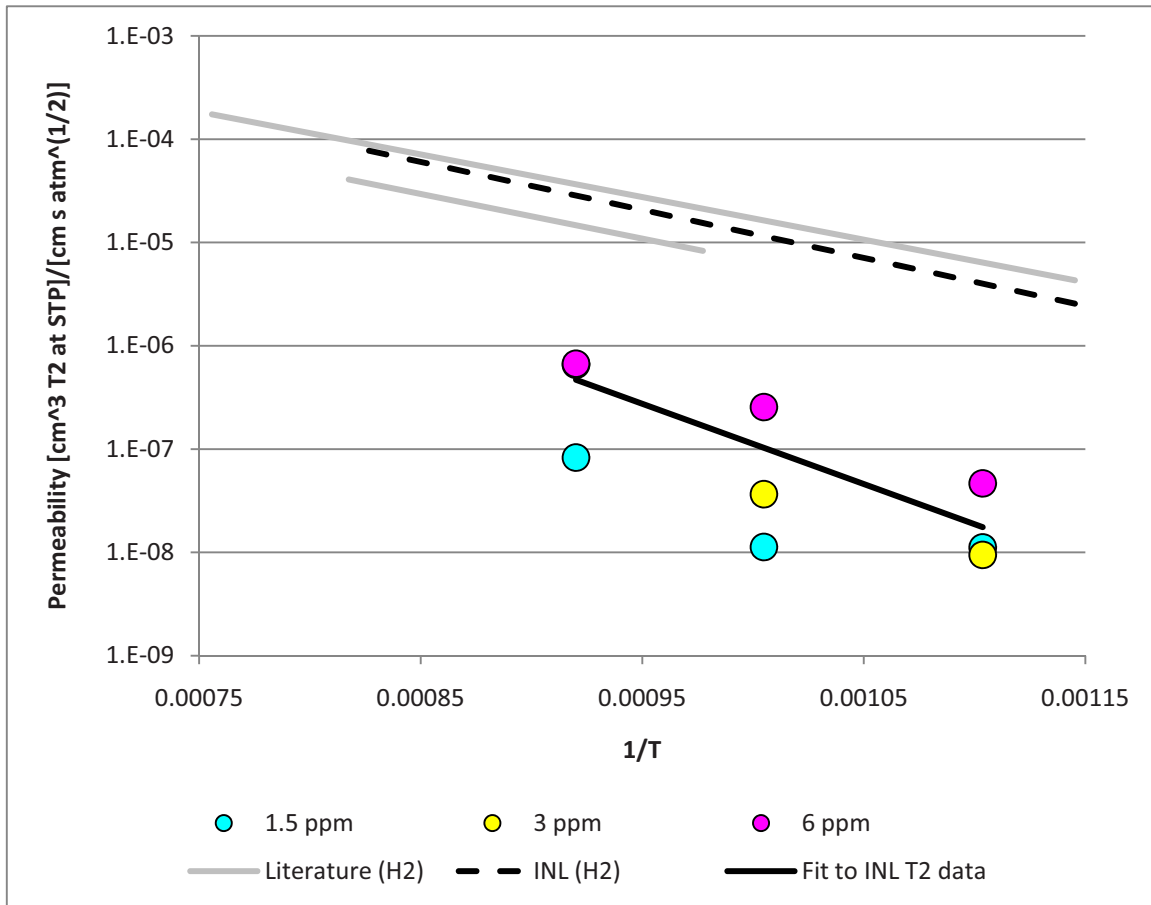
Figure 18. Arrhenius plot of Inconel 617 tritium permeability with literature data (including hydrogen and detector corrections).

The effect of both corrections is considerably higher values for permeability, though they are still far (more than an order of magnitude) below published values, and those previously obtained for hydrogen with this apparatus. The reason for this is not presently known. There are a number of complicating factors in the calculation:

V-1.   Uncertain detector response

V-2.   Insufficient in-situ monitoring of tritium activity/concentration in the primary loop

V-3.   The presence of an unknown quantity of hydrogen

V-4.   Few, and scattered, data points; moving a single data point skews the fit considerably, as evidenced by the Inconel 617 parameters in Table 7.

V-5.   Deviation from the square root of partial pressure dependence due to low tritium partial pressure

V-6.   Effects of oxide layer formation, or the formation of HTO

It is possible that there is an as-yet unidentified tritium sink in the system resulting in systematically lower calculated permeability; it is also possible that the permeation behavior is different at the very low concentrations measured here, though, in light of the aforementioned uncertainties, no such conclusion can be firmly drawn without further testing.

5. CONCLUSIONS

The design of the NGNP reactor and high-temperature components must consider the permeation of fission-generated tritium through the high-temperature components such as the heat exchanger. Loss of fission-generated tritium represents an environmental release and hydrogen contamination of the helium coolant. To support engineering design, the tritium permeability of Incoloy 800H and Inconel 617 has been measured, and compared to test values established for these materials in hydrogen permeation.

A system was designed, fabricated, and tested for measuring the permeability of metal alloys at high temperatures. The system uses counter-flow gas loops with calibrated mass flow and pressure controllers, an induction heater to heat the tubular sample to temperatures in the range 650 to 950°C, an ion chamber for measuring tritium concentration in the loops, an internal calibrated thermocouple for controlling the sample temperature, and an infrared thermal imaging system for measuring the temperature distribution in the heated sample. The operation of the system was tested and validated using hydrogen, and tritium testing was completed in FY 2011.

When operating with tritium in helium produced from mixing source gas from the Tritium Storage and Assay system, there is uncertainty regarding the concentration and uniformity of the mixture. There is an indicated offset in the permeability constant based on the values shown on the ion chamber monitor system. This offset is nominally two orders of magnitude lower than that expected from the calculated concentration when compared to the previously established hydrogen permeation values. The offset is reduced when adjustment is made for the difference between the indicated values for the secondary ion chamber and the summed activity from primary and secondary measured by the ion chamber located in the tritium recovery hood.

A significant unknown in the system response is the background concentration of hydrogen in the system. Although a nominal 15 ppm H_2 was reported for the system during hydrogen testing, definite measurement of a low concentration of hydrogen and tritium in a helium mixture is generally beyond conventional mass spectroscopy or thermal conductivity analytical techniques.[c]

There is a possibility that calibration of the ion chambers using electronic inputs and testing with a cesium-137 gamma ray source does not reflect the operating conditions. It may be necessary to acquire a helium-tritium calibration source gas to validate the ion chamber response. It may also be possible to use a gas mixture that was produced for the TMIST test program to minimize uncertainty of mixing. Rearrangement of the current system to include an ion chamber to monitor primary loop tritium concentrations is also recommended.

The system was used to measure the permeability of Incoloy 800H and Inconel 617 and at primary tritium partial pressures as low as 0.15 Pa, significantly below the hydrogen pressures used in the published data. Upper and lower bound fits were obtained for both Incoloy 800H and Inconel 617, which made different assumptions about the measured primary tritium concentration and the background hydrogen concentration, both of which influence tritium permeability. The temperature-independent permeability constant and the activation energy were determined to be as 0.01 cm^3 hydrogen (STP)/cm·sec·atm$^{1/2}$ and 25.1 kcal/mol (lower), and 0.10 cm^3 hydrogen (STP)/cm·sec·atm$^{1/2}$ and 27.1 kcal/mol (upper), for Incoloy 800H. For Inconel 617, values of 0.15 cm^3 hydrogen (STP)/cm·sec·atm$^{1/2}$ and 29.8 kcal/mol (lower), and 6.6 cm^3 hydrogen (STP)/cm·sec·atm$^{1/2}$ and 35.6 kcal/mol (upper) were obtained. The upper values for both alloys give permeabilities that are still considerably lower than

---

c. J. Giglio and W. Bauer of INL MFC Nuclear Materials Measurement and IRC Chemical and Radiation Measurement groups, personal communication.

published values in the temperature range of interest. Due to uncertainties in the measurements, it is not presently known whether this represents a real decrease in permeability at low tritium pressures.

As a result, the permeation measurements made in hydrogen should be considered the valid data set for use in any assessment until the issues associated with the tritium measurements can be resolved. If funding is available in the future the cause of the anomalous tritium permeability will be investigated.

6. REFERENCES

1. D. L. Hanson, *Test Plan for Characterizing Tritium Transport in a VHTR*, PC-000550-0, General Atomics, San Diego, CA, December 20, 2007.

2. Y. Mori, H. Ikegami, and T. Nakada, 1974, "49. High temperature helium heat exchange loop," *BNES Conference on the HTR and Process Applications, Institute of Civil Engineering, Westminster, London, November 26-28, 1974*, paper 49, pp 49.1-49.12.

3. K. Masui, H. Yoshida, and R. Watanabe, "Hydrogen Permeation through Iron, Nickel, and Heat Resisting Alloys at Elevated Temperatures," *Transactions of the Iron and Steel Institute of Japan*, Vol. 19, Issue 9, 1979, pp. 547–552.

4. H. D. Roehrig, R. Hecker, J. Blumensaat, and J. Schaefer, "50. Experimental facilities for the investigation of hydrogen and tritium permeation problems involved with steam methane reforming by nuclear process heat," *BNES Conference on the HTR and Process Applications, Institute of Civil Engineering, Westminster, London, November 26–28, 1974*, paper 49, pp 50.1-50.11. Also, H. D. Roehrig, R. Hecker, J. Blumensaat, and J. Schaefer, "Studies on the Permeation of Hydrogen and Tritium in Nuclear Process Heat Installations," *Nuclear Engineering and Design*, Vol. 34, 1975, pp. 157167.

5. A. S. Schmidt, F. Verfuss, and E. Wicke, "Studies on the permeation of hydrogen and tritium through heat resistant alloys," *Journal of Nuclear Materials*, Vol. 131, Issues 2-3, 1985, pp. 247–260.

6. T. Tanabe, S. Imoto, and Y. Miyata, "Hydrogen Permeation through Incoloy 800," *Journal of Nuclear Science and Technology*, Vol. 16, Issue 4, 1979, pp. 310–302.

7. Y. Narita, "Study on Hydrogen Permeation through Super Alloys," *Proceedings of the Japan-U.S. Seminar on HTGR Safety Technology*, Helium Technology Volume II, BNL-NUREG-50689-Vol. II, Brookhaven National Laboratory, Upton, New York, September 15–16, 1977, pp. 71–85.

8. T. Tanabe, INTOR Study Group Report (IAEA 1979), EUR FU BRU/XII 501/79/EDV 80, 1974, cited by A. D. Le Claire, "Permeation of Gases Through Solids III-As Assessment of Measurements of the Steady State Permeability of H and its Isotopes through Ni and through Several High Ni Commercial Alloys and Steels," AERE-R-10846, United Kingdom Atomic Energy Authority Harwell, March 1983.

9. H. P. Buchkremer, H. J. Cordewiner, W. Diehl, G. Esser, D. Fischmann, R. Hecker, M. Hishida, J. Lambrecht, V. Malka, R. Raitz von Frentz, H. D. Roehrig, A. Tauber, and J. Schaefer, *Ueberblick ueber die neueren Arbeiten auf dem Gebiet des Wasserstoff- und Tritiumverhaltens in Hochtemperaturreaktoren*, Juel-1497, Kernforschungsanlage Juelich, GmbH, Contributions of the Institute of Reactor Development to the II Seminar on Hydrogen and Tritium Behavior in HTRs, March 8, 1978.

10. S. Bhattacharyya, E. J. Veserly, Jr., and V. L. Hill, *Determination of Hydrogen Permeability in Uncoated and Coated Superalloys, Interim Report*, DOE/NASA/0006-1, NASA CR-165209, prepared by Illinois Institute of Technology Research Institute, Chicago, IL, for the National Aeronautics and Space Administration, Lewis Research Center, January 1981.

11. P. Calderoni and M. A. Ebner, *Hydrogen Permeability of Incoloy 800H, Inconel 617, and Haynes 230 Alloys,* INL/EXT-10-19387.

12. J. Schaefer, D. Stoever, and R. Hecker, "Terms and Results of Hydrogen Permeation Testing of Oxide-Scaled High-Temperature Alloys," *Nuclear Technology*, Vol. 66, 1984, pp. 537–549.

13. J. T. Bell, J. D. Redman, and H. F. Bittner, "Tritium Permeation through Clean Construction Alloys," *Journal of Materials for Energy Systems*, Vol. 1, 1979, pp. 55–59.

14. J. T. Bell, J. D. Redman, and H. F. Bittner, "Tritium Permeation through Clean Incoloy 800 and Sanicro 31 Alloys and through Steam Oxidized Incoloy 800," *Metallurgical Transactions A*, Vol. 11A, 1980, pp. 775–782.

15. A. Sieverts, "Über Lösungen von Gasen in Metallen," *Zeitschrift für Elektrochemie und angewandte physikalische Chemie,* Vol. 16, 1910, pp. 707-713.

16. R. A. Strehlow and H. C. Savage, "The Permeation of Hydrogen Isotopes through Structural Metals at Low Pressures and through Metals with Oxide Film Barriers," *Nuclear Technology*, Vol. 22, 1974, pp. 127–137.

17. W. M. Robertson, 1972, "Hydrogen Permeation, Diffusion and Solution in Pure Nickel and a Nickel Based Superalloy," *International Meeting on Hydrogen in Metals, Vol II, Kernforschungsanlage Juelich, Germany, March 20-24, 1972*, pp. 449–491.

18. G. R. Longhurst, G. A. Deis, P. Y. Hsu, L. G. Miller, and R. A. Causey, "Gamma Radiation Effects on Tritium Permeation Through Stainless Steel," *Nuclear Technology/Fusion,* Vol. 4, 1983, pp. 681-686.

19. S. Tosti and V. Violante, "Numerical approach for a study of the hydrogen isotopes separation by palladium alloy membranes," *Fusion Engineering and Design,* Vol. 43, 1998, pp. 93-100.

Appendix A

Summary of Incoloy 800H Permeability Data

Appendix A
Summary of Incoloy 800H Permeability Data

A total of 13 permeability measurement tests were performed with Incoloy 800H. Parameters common to all tests include the sample thickness (0.0254 cm), sample length (15.24 cm), sample inner diameter (0.635 cm), primary and secondary helium pressures (105000 Pa), and secondary helium flow rate (100 sccm). Note that wherever the terms "lower" and "upper" appear, these refer to the sets of parameters that result in lower and upper bounds on permeability, not necessarily the parameters themselves.

Table A-1. Test parameters and tritium permeation data for Incoloy 800H.

Test	Peak Temp °C	Average Temp °C	He flow rate, sccm	Primary Loop		Secondary Loop	
				T_2 Concentration, mol/m^3		T_2 Concentration, mol/m^3	T_2 Permeation Flow, mol/s
				Lower	Upper		
TS20_5	700	616	2	2.58E-04	6.22E-05	2.81E-07	4.52E-13
TS20_1	800	702	2	2.58E-04	1.64E-04	3.56E-06	5.72E-12
TS20_3	800	702	2	2.58E-04	8.65E-05	2.46E-06	3.96E-12
TS20_4	950	836	2	2.58E-04	8.92E-05	7.71E-06	1.24E-11
TS20_6	700	616	6	2.58E-04	8.02E-05	1.35E-07	2.17E-13
TS20_2	800	702	6	2.58E-04	8.59E-05	2.42E-06	3.89E-12
TS20_7	950	836	6	2.58E-04	7.98E-05	1.01E-05	1.62E-11
TS20_8	700	616	15	1.34E-04	1.03E-04	1.24E-07	2.00E-13
TS20_9	800	702	15	1.34E-04	1.03E-04	1.46E-07	2.35E-13
TS20_10	950	836	15	1.34E-04	7.03E-05	5.32E-06	8.55E-12
TS20_11	700	616	15	7.03E-05	7.34E-05	2.26E-07	3.63E-13
TS20_12	800	702	15	7.03E-05	7.57E-05	2.27E-07	3.66E-13
TS20_13	950	836	15	7.03E-05	6.53E-05	2.24E-06	3.60E-12

Table A-2. Tritium permeability coefficients for Incoloy 800H.

Test	Ave. Temp. °C	Primary T_2 Pressure, Pa		Secondary T_2 Pressure, Pa	Permeability cm^3 T_2 at STP/cm·s·atm$^{1/2}$	
		Lower	Upper		Lower limit	Upper limit
TS20_5	616	6.45E-01	1.55E-01	7.00E-04	3.72E-09	2.53E-08
TS20_1	702	6.45E-01	4.08E-01	8.88E-03	5.17E-08	1.33E-07
TS20_3	702	6.45E-01	2.16E-01	6.14E-03	3.49E-08	1.67E-07
TS20_4	836	6.45E-01	2.22E-01	1.92E-02	1.19E-07	5.41E-07
TS20_6	616	6.45E-01	2.00E-01	3.37E-04	1.77E-09	9.55E-09
TS20_2	702	6.45E-01	2.14E-01	6.03E-03	3.43E-08	1.65E-07
TS20_7	836	6.45E-01	1.99E-01	2.52E-02	1.61E-07	8.24E-07
TS20_8	616	3.35E-01	2.57E-01	3.10E-04	2.28E-09	6.95E-09
TS20_9	702	3.35E-01	2.56E-01	3.64E-04	2.68E-09	8.17E-09
TS20_10	836	3.35E-01	1.75E-01	1.33E-02	1.18E-07	4.61E-07
TS20_11	616	1.75E-01	1.83E-01	5.63E-04	5.88E-09	1.74E-08
TS20_12	702	1.75E-01	1.89E-01	5.67E-04	5.92E-09	1.70E-08
TS20_13	836	1.75E-01	1.63E-01	5.59E-03	6.70E-08	1.99E-07

Appendix B

Summary of Inconel 617 Permeability Data

Appendix B
Summary of Inconel 617 Permeability Data

A total of 9 permeability measurement tests were performed with Inconel 617. Parameters common to all tests include the sample thickness (0.0254 cm), sample length (15.24 cm), sample inner diameter (0.635 cm), primary and secondary helium pressures (105000 Pa), primary helium flow rate (15 sccm), and secondary helium flow rate (100 sccm). Note that wherever the terms "lower" and "upper" appear, these refer to the sets of parameters that result in lower and upper bounds on permeability, not necessarily the parameters themselves.

Table B-1. Test parameters and tritium permeation flow data for Inconel 617.

Test	Peak Temp °C	Average Temp °C	Primary Loop		Secondary Loop	
			T_2 Concentration, mol/m^3		T_2 Concentration, mol/m^3	T_2 Permeation Flow, mol/s
			Lower	Upper		
TS17_1	700	625	2.68E-04	1.73E-04	1.33E-06	2.14E-12
TS17_2	800	713	2.68E-04	1.65E-04	6.74E-06	1.08E-11
TS17_3	900	804	2.68E-04	1.44E-04	1.46E-05	2.34E-11
TS17_4	700	625	1.26E-04	8.87E-05	1.47E-07	2.37E-13
TS17_5	800	713	1.26E-04	8.07E-05	5.19E-07	8.36E-13
TS17_6	900	804	1.26E-04	5.78E-05	6.06E-06	9.75E-12
TS17_7	700	625	2.58E-04	7.38E-05	1.46E-07	2.35E-13
TS17_8	800	713	1.34E-04	7.30E-05	1.46E-07	2.35E-13
TS17_9	900	804	1.34E-04	7.97E-05	1.15E-06	1.85E-12

Table B-2. Tritium permeability coefficients for Inconel 617.

Test	Ave. Temp. °C	Primary T_2 Pressure, Pa		Secondary T_2 Pressure, Pa	Permeability cm^3 T_2 at STP/cm·s·atm$^{1/2}$	
		Lower	Upper		Lower limit	Upper limit
TS17_1	625	6.68E-01	4.32E-01	3.32E-03	1.81E-08	4.66E-08
TS17_2	713	6.68E-01	4.11E-01	1.68E-02	1.01E-07	2.55E-07
TS17_3	804	6.68E-01	3.59E-01	3.64E-02	2.39E-07	6.71E-07
TS17_4	625	3.14E-01	2.21E-01	3.67E-04	2.80E-09	9.47E-09
TS17_5	713	3.14E-01	2.01E-01	1.30E-03	1.02E-08	3.67E-08
TS17_6	804	3.14E-01	1.44E-01	1.51E-02	1.43E-07	6.56E-07
TS17_7	625	6.45E-01	1.84E-01	3.64E-04	1.92E-09	1.12E-08
TS17_8	713	3.35E-01	1.82E-01	3.64E-04	2.68E-09	1.13E-08
TS17_9	804	3.35E-01	1.99E-01	2.87E-03	2.25E-08	8.29E-08